

Article

# A Novel Composite Index to Measure Environmental Benefits in Urban Land Use Optimization Problems

Md. Mostafizur Rahman <sup>1,2,\*</sup> and György Szabó <sup>1</sup>

<sup>1</sup> Department of Photogrammetry and Geoinformatics, Faculty of Civil Engineering, Budapest University of Technology and Economics, 3 Műegyetem rkp., K Building First Floor 31, H-1111 Budapest, Hungary; szabo.gyorgy@emk.bme.hu

<sup>2</sup> Department of Urban and Regional Planning, Rajshahi University of Engineering and Technology, Rajshahi 6204, Bangladesh

\* Correspondence: rahman.mostafizur@emk.bme.hu; Tel.: +36-202300148

**Abstract:** In urban land use optimization problems, different conflicting objectives are applied. One of the most significant goals in urban land use optimization problems is to maximize environmental benefits. To quantify environmental benefits in land use optimization, many researchers have employed a variety of methodologies. According to previous studies, there is no standard approach for calculating environmental benefits in urban land use allocation problems. Against this background, this study aims to (a) identify indicators of environmental benefits and (b) propose a novel composite index to measure environmental benefits in urban land use optimization problems. This study identified four indicators as a measure of environmental benefits based on a literature assessment and expert opinion. These are spatial compactness, land surface temperature, carbon storage, and ecosystem service value. In this work, we proposed a novel composite environmental benefits index (EBI) to quantify environmental benefits in urban land use allocation problems using an ordered weighted averaging (OWA) method. The study results showed that land surface temperature (LST) is the most influential indicator of environmental benefit while carbon storage is the least important factor. Finally, the proposed method was applied in Rajshahi city in Bangladesh. This study identified that, in an average-risk decision, most of the land (64.55%) of the study area falls within the low-environmental-benefit zone due to a lack of vegetated land cover. The result suggests the potential of using EBI in the land use allocation problem to ensure environmental benefits.

**Keywords:** spatial compactness; land surface temperature; ecosystem service value; carbon storage; environmental benefits index



**Citation:** Rahman, M.M.; Szabó, G. A Novel Composite Index to Measure Environmental Benefits in Urban Land Use Optimization Problems. *ISPRS Int. J. Geo-Inf.* **2022**, *11*, 220. <https://doi.org/10.3390/ijgi11040220>

Academic Editor: Wolfgang Kainz

Received: 8 January 2022

Accepted: 21 March 2022

Published: 23 March 2022

**Publisher's Note:** MDPI stays neutral with regard to jurisdictional claims in published maps and institutional affiliations.



**Copyright:** © 2022 by the authors. Licensee MDPI, Basel, Switzerland. This article is an open access article distributed under the terms and conditions of the Creative Commons Attribution (CC BY) license (<https://creativecommons.org/licenses/by/4.0/>).

## 1. Introduction

Land use optimization is an important technique for attaining sustainable urban development through environmental protection, efficient resource use, economic prosperity, and social equity [1–3]. It acts as a decision support system for land use decisions and considers many criteria to reach the ultimate decision. There are certain conflicting interests in urban land use optimization since multiple stakeholders are involved in the optimization process. If residential growth develops in a low-lying location, for example, it may address the housing problem, but it may exacerbate the urban drainage issue. If green space is replaced by urban buildings, the urban environment and health would suffer as a result of urbanization. While property developers seek to maximize their financial earnings, the government seeks to maximize the social advantages of land use allocation. In urban land use optimization games, different conflicting objectives are considered. Some of the objectives are widely employed in urban land use optimization. The maximization of economic benefits, maximization of ecological benefits, maximization of environmental benefits, minimization of land conversion costs, maximization of land value, maximization

of land use compatibility, maximization of accessibility, maximization of compactness, maximization of ecosystem service value (ESV), and maximization of social benefits are some of the most important objectives. [4].

One of the most significant goals in urban land use optimization problems is to maximize environmental benefits. Cities around the world are confronted with a variety of environmental challenges, including air, water, and soil pollution, traffic and noise congestion, and poor housing conditions, in the face of unsustainable urban development and climate change [5]. Rapid urban growth has exacerbated the environmental problems associated with the unsustainable management of transport, housing, waste, energy, and land use [6]. Cities play an important role in environmental change. For example, cities are responsible for over 75% of worldwide greenhouse gas emissions. Urban areas also produce large volumes of trash, much of which is inadequately handled and poses a health risk to people and ecosystems [7]. The structure and composition of urban land use affect the urban environment, ecosystem, and biodiversity in many ways. Due to the high population density and urbanization, especially in developing countries, urban land uses are changing. The majority of such land use changes are detrimental to the natural ecosystem, particularly in terms of farmland loss [8], air and water pollution, the urban heat island effect [9], surface runoff, habitat variety, and biodiversity loss [10]. For example, the expansion of the urban impervious surface due to urbanization affects the city's overall thermal climate. Due to the rapid urbanization and population growth, the urban vegetation, agricultural land, and wetland are being occupied by built environment, e.g., residential, commercial, and industrial activities. These changes deteriorate the urban environment and ecosystem [11]. When recognizing and anticipating future urban environmental challenges, urban sustainability becomes the global concern among top-level decision makers as well as academics and researchers. In recent times, the quality and benefits of the urban environment have become the focus of scientific research and a hot topic of researchers in related fields. For example, Javanbakht et al. [12] presented an approach to the spatial-temporal mapping of urban air quality based on fuzzy logic, an analytical network process, remote sensing imagery, and field-collected data. Hsueh and Lin [13] identified different dimensions of urban environmental benefits. Their study found that health, sustainability, security, awareness, and convenience are the five most critical dimensions of urban environmental benefits. Mishra et al. [14] developed a novel tool to assess the urban environmental benefits of urban green and blue spaces. It is widely acknowledged that globally significant socioeconomic progress and rapid urbanization in the past decades occurred at the expense of natural and urban environmental quality and benefits. The scenario is more prevalent in developing countries. As a result, it becomes a global concern to focus on finding the solution that can ensure both socioeconomic development and environmental sustainability [15,16].

Against this background, many researchers have considered maximizing environmental benefits in urban land use optimization problems to ensure urban environmental sustainability. However, according to our earlier study [4], we found no established technique to compute the environmental benefits in land use allocation problems. Early studies in urban land use optimization problems used different methods to measure environmental benefits in urban land use allocation. For example, Yuan et al. [17] used carbon storage as the proxy for measuring environmental benefits, assuming that carbon storage can contribute to maintaining air pollution. Spatial compactness as a measure of environmental benefits has also been used in many studies, assuming that a compact city is more sustainable and livable [18], provides better accessibility to city facilities and promotes public health and living [19], and can maximize the overall environmental benefits of the people [20]. However, we contend that a single metric may not be the best way to assess environmental benefits. Rather a set of multiple indicators can best describe the environmental benefits in an urban area. Therefore, a composite index is needed to assess environmental benefits. However, according to our previous study [4], we found no such

proven approach to assess environmental benefits in the land use allocation field. Although some studies considered multiple indicators to measure environmental benefits, those studies did not consider only land use allocation. For example, Lin [13] identified five critical indicators of urban environmental benefits. These indicators are health, sustainability, security, awareness, and convenience. However, these indicators are not completely related to urban land use allocation. We believe that the spatial composition and structure of urban land use allocation have an impact on urban environmental benefits and that the different aspects and attributes of urban land use can be used to measure urban environmental benefits. Against this background, this study aims to (a) identify the appropriate indicators of environmental benefits and (b) propose a composite index to measure environmental benefits in urban land use allocation. In Section 2, we have presented the literature review for understanding the indicators of urban environmental benefits. Based on the literature review, we have identified nine indicators of urban environmental benefits, which are presented in Table 1. Among these nine indicators, four indicators are the most important: (a) spatial compactness, (b) ecosystem service value (ESV), (c) land surface temperature (LST), and (d) carbon storage. These four indicators are predominant over the others because these indicators also represent other indicators in Table 1. For example, LST is the main basis of the urban heat island effect [9,21], carbon storage (including soil carbon) is also related to air pollution and soil pollution [22,23], and ESV represents the effect of urban farming [24,25]. Using these indicators, we have developed an environmental benefits index (EBI) using the multi-criteria evaluation (MCE) method. This study is unique in the sense that this study proposed a composite index based on only the attributes of urban land use.

**Table 1.** Indicators of environmental benefits in land use allocation.

Indicators	References
Spatial compactness	[2,18,19,26–31]
Land surface temperature	[32–38]
Ecosystem service value	[39–46]
Carbon storage	[22,23,47–56]
Air pollution	[57–65]
Soil pollution	[66–74]
Urban farming	[75–81]
Urban heat island effects	[82–87]
Urban flooding	[88–93]

Source: Prepared by the authors based on a literature review and expert opinion.

The rest of the paper has been structured as follows: Section 2 describes the relevant literature. This section discusses the different indicators used in different studies as measures of environmental benefits in urban land allocation. Section 3 describes the data used in this study and the methods followed for constructing the EBI. This section describes the detailed procedure to calculate each indicator used to develop the EBI. The method to calculate the weight of each indicator is also described in this section. The result of this study is presented in Section 4. This section illustrates the output of the EBI indicators and the development of the EBI. The discussion of the findings is also illustrated in this section. Finally, this paper ends with Section 5, which contains the concluding remarks of this study.

## 2. Literature Review

Urban land use planning has a significant impact on urban environmental benefits. The compositions and spatial patterns of urban land uses are diverse. The compositions and spatial patterns of land use affect the urban environment in many ways. Concerning the compositions and spatial patterns of urban land uses, many indicators are contributing to urban environmental benefits. This section discusses the different types of indicators that can be used to measure environmental benefits from urban land use allocation. At the end of the section, we have summarized the list of possible indicators of environmental benefits based on the literature review.

Spatial compactness has been used in many land use optimization problems with the argument that a compact city results in many environmental benefits [2,17,29,31]. In many urban land use optimization situations, the maximization of spatial compactness has been employed as one of the optimization objectives, according to a comprehensive review by Rahman and Szabó [4]. In previous studies, spatial compactness was used as an indicator of urban environmental benefits since there are numerous perceived advantages of compact cities over urban sprawl, including lower car dependency and, thus, lower emissions, reduced energy consumption, improved public transportation services, increased overall accessibility, the re-use of infrastructure and previously developed land, the regeneration of existing urban areas and urban vitality, a higher quality of life, the preservation of green space, and the creation of an environment conducive to enhanced business and trading activity [18,19,26,30,31]. All these benefits are urban environmental benefits related to spatial compactness. While spatial compactness in the city has many environmental benefits, other studies suggest that it can also lead to lower living space, less access to natural spaces, less affordable housing, and poorer health [94]. Traffic congestion in the city center might result in increased emissions and noise pollution due to a higher level of spatial compactness [95]. Other researchers believe that the harmful impact of the compact city on health is more severe because of the high concentration of emissions in the inner city [96]. Therefore, other variables should be considered in addition to spatial compactness when measuring environmental benefits in urban land allocation. Different methods were used to measure urban spatial compactness. The most common methods used to measure spatial compactness included (a) the non-linear integer program-neighbor method, (b) the linear integer program-neighbor method, (c) the minimization of the shape index, (d) linear IP using aggregated blocks/minimization of the number of clusters per land use type, (e) a linear integer program using buffer cells, and (f) spatial autocorrelation [97–100]. The non-linear integer program is the simplest explanation for land use compactness, as it relies solely on the neighbors of each cell to calculate the compactness by sum. The linear integer program model is an analogous linear reformulation of the first with the inclusion of integer variables [101]. The minimization of the shape index method calculates each cluster's form index, which sounds complicated but is a good way to describe compactness [102]. The fourth concept is to group individual cells into blocks and create a model that reduces the number of blocks in the final allocation result that contains only one land use category. In other words, the goal is to reduce the number of clusters by as much as possible for each land use category. The fifth method was stated as a problem in which parcels are chosen and each reserve (one land use type) is divided into core cells and a buffer zone. Compactness is achieved indirectly by reducing the number of buffer cells surrounding the core sections [103]. The last option is to use Moran's I and other geographical statistics to calculate the spatial compactness [104].

LST is a key indicator of the environment and climate in cities [105–107]. LST is one of the important factors controlling the urban environment. On the other hand, urban LST mostly depends upon the composition and dynamics of urban land cover [108]. For example, the surface temperature in urban areas is higher than in vegetated and water-covered areas because of the surface cover. Since the composition of the urban land surface, mostly in developing countries, has been experiencing changes, including

conversion to more built-up areas, due to rapid urbanization, the urban LST is also rising [109,110]. The increase in temperature is also deteriorating the urban environment. Therefore, it is very important to consider LST in urban land allocation problems because it affects the overall urban environment. Since LST can affect urban environmental benefits, many studies incorporated LST in urban environmental analyses. For example, a study by Santamouris [111] showed that increased LST has a significant impact on cooling energy use, heat-related mortality and morbidity, urban environmental quality, local vulnerability, and thermal comfort. Xue et al. [112] considered temperature as one of the environmental factors to estimate the association between the environment and mental health. Their study suggested that an increase in temperature is associated with higher probabilities of declined mental health. Yu et al. [113] studied the effect of urban land use zoning on the urban heat island effect. Their study showed that the composition of urban land cover and functional zoning significantly contribute to LST and the urban environment.

Urban ecosystem services play an important role in connecting cities with the biosphere and reducing the ecological footprint and ecological debt of cities while at the same time enhancing urban environmental quality, public health, resilience, and the quality of urban life [114]. Urban ecosystem services contribute directly or indirectly to human well-being, providing many functions, including the food supply, water supply, waste treatment, regulation of the urban heat island effect, clean air, water filtration, noise reduction, pollination, climate regulation, etc. [37,39,40]. Most of these functions are strongly related to urban environmental benefits. Ecosystem services could contribute to the urban environment in many ways. A healthy ecosystem can also ensure urban environmental sustainability and contribute to achieving sustainable development. On the other hand, a vulnerable urban ecosystem will lead to environmental pollution, biodiversity decline, land degradation, and extreme climatic events, develop the urban heat island effect, and threaten public health, human safety, and global ecological security [41,47,115]. Thus, researchers and urban policymakers are interested in monitoring the health of urban ecosystem services and understanding their relationship with human well-being in cities to support coordinated urban development that benefits social interests, the urban economy, and the environment [116,117]. Urban ecosystem services are strongly influenced by the composition of urban land use and land cover (LULC) and their spatio-temporal dynamics. Considering the importance of ecosystem service to maintaining the urban environment and its nexus with urban LULC, many researchers studied the impact of LULC change on ESV. For example, Lin et al. [41] examined the influence of LULC changes on ecosystem service in Chengdu city, China; Hein et al. [118] analyzed the spatial scale of ecosystem services and studied how stakeholders assign value to different ecosystem services based on the spatial scale; Tolessa et al. [45] monitored the impact of land use/land cover change on ecosystem services in the central highlands of Ethiopia. Estoque and Murayama [119] examined the potential impact of LULC change on the ecosystem services of Baguio city, the Philippines, and observed a substantial decrease in ESV due to the change of agricultural and forest land to built-up areas.

Climate change is wreaking havoc on our world, generating extreme weather events, such as tropical storms, wildfires, severe droughts, and heat waves, as well as significantly affecting food output and disrupting animal habitats. Because greenhouse gas emissions are the primary driver of global warming and, thus, climate change, carbon storage plays an important role in mitigating the effect of greenhouse gas emission and controlling the environment and climate [23,49]. Carbon storage is associated with controlling the environment in many ways. Carbon storage can reduce the emissions of different types of gaseous pollutants responsible for environmental pollution. For example, studies show that emissions due to sulfur dioxide (SO<sub>2</sub>), particulate matter (PM), nitrogen oxide (NO<sub>x</sub>), and ammonia (NH<sub>3</sub>) are significantly reduced by carbon storage [50,54,56]. There is a strong correlation and a high degree of spatial congruence

between carbon storage and environmental quality [120]. Carbon storage is critical not only for today's communities and habitats but also for future generations of people, plants, and animals. If enough carbon is sequestered and emissions are reduced, the greenhouse effect will be lessened in the future, resulting in fewer warm days and fewer droughts and other extreme weather events linked to climate change. Due to the significance of carbon storage in maintaining urban environmental quality, many researchers focused on analyzing carbon stock assessment, an impact of forestry, vegetation, and land cover change on carbon storage. For example, Nowak et al. [54] quantified carbon storage and sequestration by urban trees in the United States to assess how urban forests contribute to climate change and the overall environment. In their study, they assessed the carbon density based on the density of urban trees and found that the density of carbon storage densities was on average 7.69 kg C/m<sup>2</sup> in urban trees in selected US cities. Adelisardou et al. [56] assessed the spatiotemporal impacts of land use/cover change (LUCC) on the provision and value of the carbon storage and sequestration in the Jiroft plain, Iran. Their study suggested that agriculture and urban expansion led to a considerable decrease in carbon storage, mainly due to rapid deforestation. The study by Ma et al. [52] showed that urban land use planning, the degree of urbanization, and the urban forest structure affect the spatial distribution of carbon storage.

Based on the literature review, we have identified several indicators that can be used to measure the environmental benefits of urban land use optimization.

### 3. Data and Methods

#### 3.1. Study Area

Rajshahi city of Bangladesh was selected as a case study for this research. This city was mainly selected for two reasons: (a) the availability of updated data and (b) this city is similar to other cities of Bangladesh so it can be considered as a representative city in the country. It can also be mentioned that although Rajshahi city of Bangladesh was selected as a case study, the approach and result of this study can be used in other cities and countries. Rajshahi city lies between 24°20'57.03" to 24°20'58.40" north latitude and 88°32'30.19" to 88°40'08.76" east longitude. The city sits on the north bank of the Padma River, which runs through the city's southern side. The city is about 243 km from the capital city, Dhaka, and is close to the India–Bangladesh border. The area and population of this city are 48.05 Km<sup>2</sup> (Figure 1) and 0.76 million, respectively [121]. The city's topography is mostly flat, with a mean surface height of 21.289 m above sea level. Rajshahi is a significant administrative, educational, cultural, and business center. Due to the higher number of educational institutions and a large number of students, the city is called an educational city of Bangladesh. The divisional headquarter is situated in this city. Rajshahi has a tropical wet and dry climate according to the Köppen climatic classification [122]. Rajshahi's climate is characterized by monsoons, high temperatures, considerable humidity, and moderate rainfall [123].

The city's first formal master plan, within the jurisdiction of the Rajshahi metropolitan area (RMA), was produced in 2004 to guide the city's future land use growth [124]. Every five years, this plan was expected to be updated to accommodate essential changes and ensure planned development. The plan, however, was not updated on time due to a lack of sufficient expertise, resources, and regulation, resulting in the unplanned expansion of the city. Recognizing the need, the Rajshahi Development Authority (RDA) has taken the initiative to amend the land use plan to ensure the city developments in a guided manner.

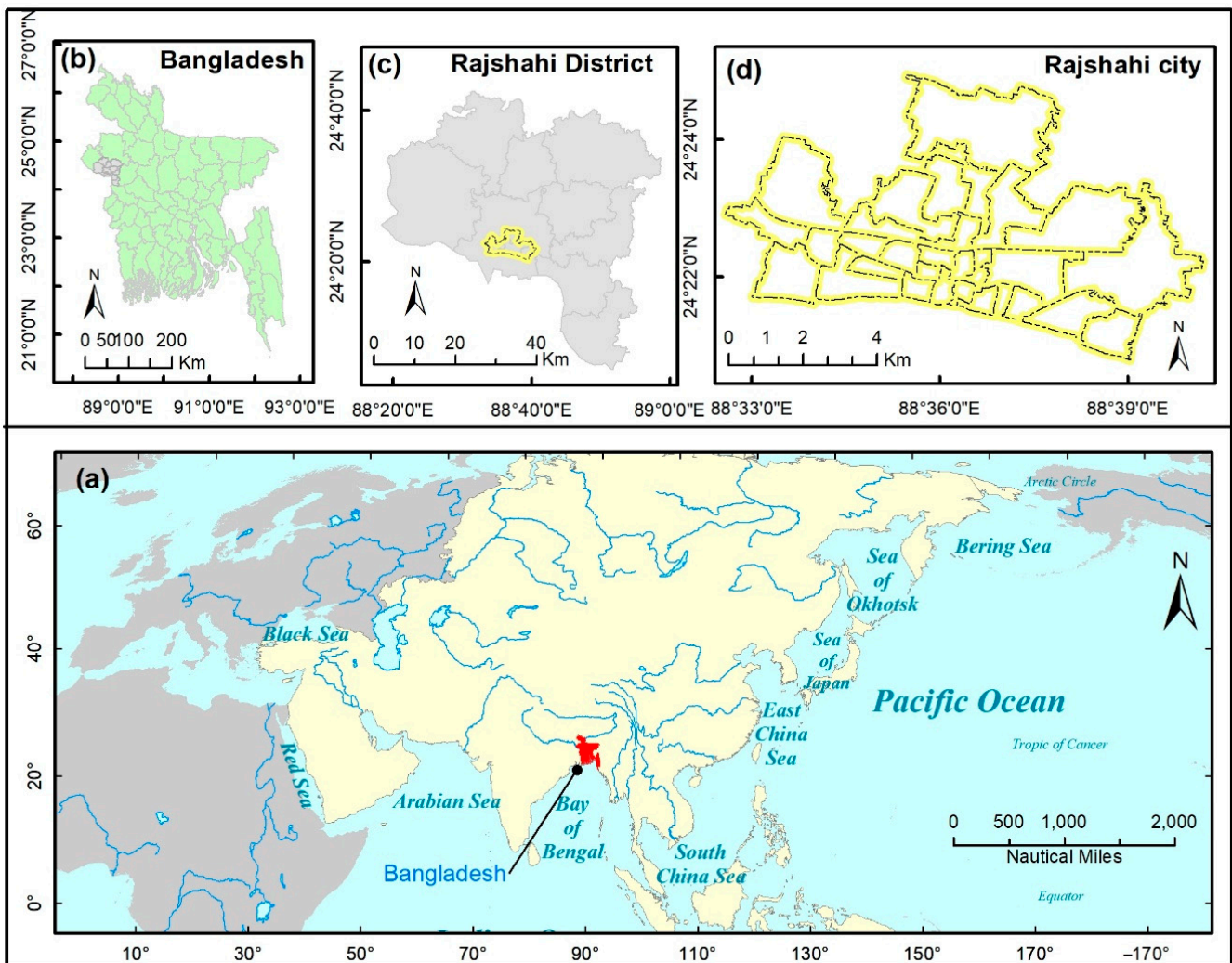


**Figure 1.** (a) Location of Bangladesh in Asian; (b) Location of the Rajshahi district with respect to Bangladesh; (c) Location of the study area with respect to the Rajshahi district; (d) Administrative boundary of the study area.

### 3.2. Data

The primary purpose of this research was to create a composite index that can be used to assess the environmental benefits of urban land use allocation. Primary and secondary data were used to achieve the goal of the study. As mentioned at the end of the introduction section, four indicators were used to develop the EBI. Spatial compactness was calculated from the spatial distribution of existing land use. These land use data were collected from the RDA of Bangladesh. The existing land use map is presented in Figure 2. The land use types include residential, commercial, and industrial areas, green spaces, educational institutions, health facilities, and water bodies.

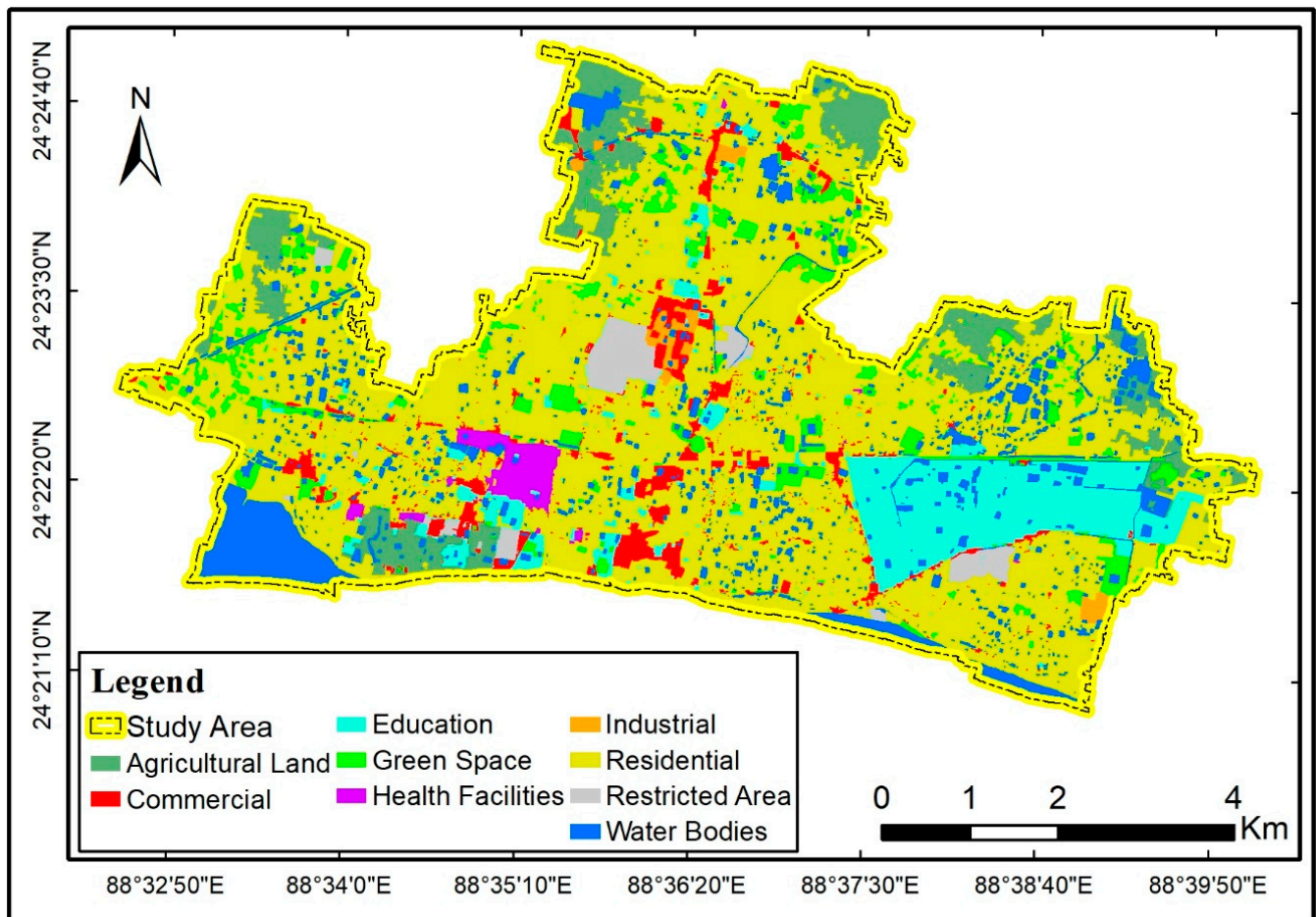


**Figure 2.** Spatial distribution of different land use types in this study area.

The ESV and LST were derived from Landsat images of 2021. To calculate carbon storage, Landsat images and secondary data were used. Landsat 8 images from the year 2021 were downloaded from the US Geological Survey (USGS) official website (<https://earthexplorer.usgs.gov/>, accessed on 19 October 2021), providing level-1 precision and terrain-corrected (L1TP) and cloud-free multispectral images. The raw images contain a digital number (DN) value for each pixel. These DN values were used for further processing of the images. A detailed method to calculate these indicators is described in the subsequent sections. Table 2 presents the detailed description of the Landsat images used in this study.

**Table 2.** Particulars of the Landsat images used in this study.

Landsat Scene ID	Acquisition Date	Satellite	Sensor	Path/Row
LC81380432021115LGN00	25/04/2021	Landsat 8	OLI/TIRS	138/43

OLI = operational land imager, TIRS = thermal infrared sensor.

The whole study area lies at the intersection of Landsat path 137 and row 44. The downloaded images had a built-in projection system of the Universal Transverse Mercator (UTM) projection within Zone 46 North based on the World Geodetic System (WGS) 1984 datum. The spatial resolution of the images used for this study was  $30 \times 30$  m per pixel. To process and calculate the indicators, ArcGIS 10.8 and TerrSet v19.0 software were used.

### 3.3. Methods

This section describes the detailed methodology of the study. Since the study encompasses a variety of data and methods, we have first illustrated the overall methodology using a flowchart in Figure 3. Then we have described the methodology.

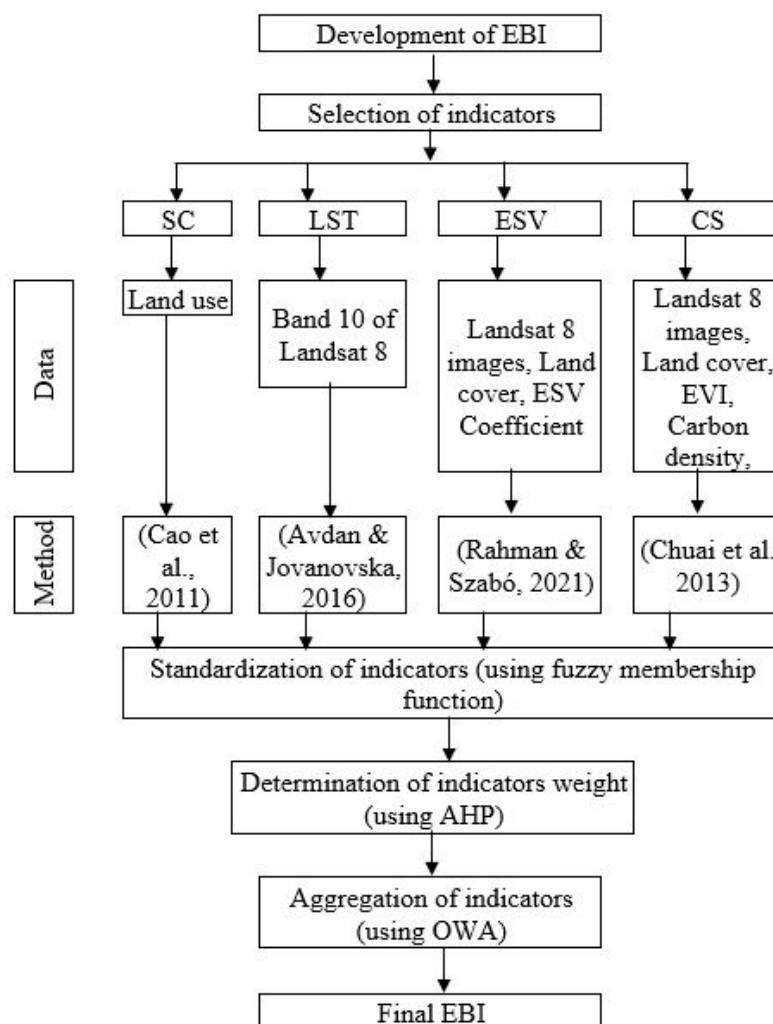


**Figure 3.** Flowchart of the overall methodology of the study.

#### 3.3.1. Indicator Selection

To create a composite index of environmental benefits, appropriate indicators that reflect environmental benefits from land use allocation must be identified. First, a literature review was undertaken to identify the indicators that can be used as measures of environmental benefits from urban land use allocation. We identified several indicators, based on the literature review, that can be used to quantify environmental benefits. The initial list of indicators was presented in Table 1. However, all the indicators are not equally important. To select the most suitable indicators, the results of the literature review were then shared with a group of 15 professionals, including environmental experts, urban planners, and ecologists. The result of the literature review was shared with the experts with the hope that the experts would reach a consensus on the indicators' benefits. Based on the literature review and experts' judgment, final indicators were selected.

#### 3.3.2. Computing the Value of Indicators

We identified four indicators as a measure of environmental benefits in land use optimization problems based on a literature review and expert opinion. These indicators

are (a) spatial compactness; (b) ecosystem service value; (c) land surface temperature; and (d) carbon storage. The method for computing those indicators is described in the following sections.

### Spatial Compactness

Urban land uses are organized in a variety of ways. Spatial compactness refers to the degree to which urban land use is structured and distributed compactly instead of sprawling. In the literature, there are several ways to measure spatial compactness, of which the non-linear IP-neighbor technique and shape index minimization are the most common and straightforward. Computation of the shape index is based on patches of the land parcel [125], and computation of the non-linear IP-neighbor method is based on Moore's eight-cell neighborhood method [126]. In this study we used Moore's eight-cell neighborhood method, due to its suitability and simplicity, to compute the spatial compactness of urban land allocation. In this method, spatial compactness is represented by the number of cells allocated for the same use in each cell's eight neighboring cells (Equation (1)) [1].

$$\text{Spatial compactness} = \sum_{k=1}^K \sum_{i=1}^N \sum_{j=1}^M b_{ijk} x_{ijk} \quad (1)$$

where

$$b_{ijk} = x_{i-1jk} + x_{i+1jk} + x_{ij-1k} + x_{ij+1k} + x_{i-1j-1k} + x_{i-1j+1k} + x_{i+1j-1k} + x_{i+1j+1k}$$

In the above Equation (1),  $K$  is the number of land use types, and  $K = 5$ .  $N$  and  $M$  are the total numbers of rows and columns of the planning area, respectively, and  $N = M = 30$ . When a cell  $(i, j)$  is allocated for land use  $k$ ,  $x_{ijk} = 1$ ; otherwise,  $x_{ijk} = 0$ . After calculating the spatial compactness for every cell, we can calculate the total compactness of a land use allocation scenario by adding the compactness of each cell under study.

### Land Surface Temperature

In this study, we have used TIRS band 10 of the Landsat image to derive the LST in the study area. The detailed method of calculating the LST from Landsat images is available in the literature. We have used the methods developed by Avdan and Jovanovska [127] and Z. Zhao et al. [128] to derive the LST in the study area. Since temperature retrieval is a well-known phenomenon that may readily be generated using an earlier method, we are not going to describe the detailed method here.

### Calculation of the ESV

The ESV was calculated based on the land cover of the study area. The land cover map was derived from the Landsat images. To calculate the ESV of the study area, two major steps were followed: (a) land cover classification from the Landsat images and (b) calculation of the ESV from the land cover image [129]. The detailed method of land cover classification was described in our earlier study [129]. Therefore, we are not going to repeat the steps here. Interested readers can have a look at our earlier paper for a detailed method. In short, the land cover classification from the Landsat images was described here. First, we processed the raw Landsat image with a DN. A three-step procedure was performed to convert the DN values to surface reflectance through a radiometric correction. These steps were (a) the conversion of the DN values to the spectral radiance at the sensor, (b) the conversion of the spectral radiance to the reflectance at the sensor, and (c) the atmospheric correction and conversion of the sensor reflectance to the surface reflectance.

In the second step, we classified the surface reflectance value to derive the land use land cover map of the study area. We used an unsupervised k-means clustering method to classify the Landsat images into five broad land cover classes. These land cover classes are (a) built-up area, (b) vegetation, (c) bare land, (d) waterbody, and (e) agricultural land. The definition of these land cover classes is presented in Table 3.

**Table 3.** Description of land cover types.

Land Cover Type	Description
Built-up Area	Urban, residential, commercial, industrial, and mixed-use areas, settlements, transport, and other man-made structures
Waterbody	River, lake, pond, canal, low land, wetland, etc.
Vegetation	Trees, mixed forest, natural vegetation, gardens, parks, playgrounds, etc.
Bare Land	Open space, construction sites, fallow land, land surface without vegetation, sand, transitional areas, bare soil, etc.
Agricultural Land	Cropland and pastures, orchards, groves, nurseries, and other agricultural lands.

After the classification was complete, it was necessary to assess the accuracy of the classified images. The Google Earth platform was used to assess the accuracy of the classified images. For accuracy assessment, the classified images were compared to the appropriate land cover in Google Earth. About 30 sample points were selected for each land cover category for accuracy assessment. Using the stratified sampling approach in ArcGIS 10.8, we generated 175 random sampling points for the accuracy assessment. The accuracy assessment showed that the overall classification accuracies of the classified images were 88.00%, with kappa coefficients of 0.859.

In the final step, the ESV was calculated based on the land cover types. Different methods were used to estimate the ESV from the land cover class. However, the benefits transfer method (BTM), developed by Costanza et al. [130], is considered as a robust method to calculate the ESV from land cover. To obtain the values of the ecosystem services for each of the 5 land cover categories in Rajshahi city, we compared the 5 categories of land cover with the 16 biomes identified in Costanza et al. [130]. The most relevant biome for each category was assigned as the proxy for that land cover type. For example, the ‘cropland’ biome for ‘agricultural land’, ‘lake/rivers’ for ‘water body’, ‘tropical forest’ for ‘vegetation’, ‘urban’ for ‘built-up area’, and ‘desert’ for ‘bare land’ were assigned for the proxy to calculate the value of ecosystem service for each land use type. Although the land cover categories and equivalent biomes did not perfectly match, their use proved feasible in many other studies [131]. Land cover types, equivalent biomes, and the corresponding value coefficients are presented in Table 4.

**Table 4.** Biome equivalents for the five land-use categories and the corresponding ecosystem values (1994 USD ha<sup>-1</sup>yr<sup>-1</sup>).

Land Cover Types	Equivalent Biome	ESV Coefficient (USD ha <sup>-1</sup> yr <sup>-1</sup> )	
		Original Value (1994)	Adjusted Value (2021)
Agricultural land	Cropland	92	171
Water body	Lakes/Rivers	8498	15,806
Vegetation	Tropical forest	2007	3733
Built-up area	Urban	0	0
Bare land	Desert	0	0

The original ESV coefficient was determined according to the 1994 USD. In our study, we adjusted the ESV coefficient considering the consumer price index (CPI) inflation rate. The CPI inflation rate in USD in 2021 with respect to the CPI in 1994 is 1.86 [132]. Thus, we multiplied the original ESV coefficient by 1.86 to calculate the adjusted ESV coefficient in 2021. This adjusted coefficient was used to calculate the ESV. Finally, the ESV for the study area was calculated using Equation (2) [133,134].

$$ESV = \sum(A_k \times VC_k) \quad (2)$$

where  $ESV$  is the total estimated value of ecosystem service,  $A_k$  is the area in hectares, and  $VC_k$  is the  $ESV$  value coefficient ( $USD\ ha^{-1}yr^{-1}$ ) for each land cover category, ' $k$ '.

#### Calculation of Carbon Storage

The carbon storage for different land types is determined by two factors: (a) above-ground carbon storage and (b) below-ground carbon storage. Above-ground carbon storage depends upon the concentration of vegetation, and below-ground carbon storage depends upon the density of soil organic carbon (SOC) [135]. Carbon storage from different land cover types was calculated using the following Equation (3) [136].

$$T = \sum_{i=1}^n T_i = A_i(V_i + S_i) \quad (3)$$

where  $T$  is the total carbon storage of the terrestrial ecosystem in the study area,  $T_i$  is the carbon storage of land use type  $i$ ,  $A_i$  is the area of land use type  $i$ , and  $V_i$  and  $S_i$  are the carbon densities of vegetation and soil of land use type  $i$ , respectively. The densities of SOC were collected from secondary sources and are presented in Table 5.

**Table 5.** Density of SOC (%) in different land cover types.

Land Cover Type	% SOC (ton/ha)	Source
Agriculture	17.608	[137,138]
Vegetation	31.24	[137]
Water	5.2	[139]
Bare Land	11.36	[137]
Built-up	9.8	[140]

Since the density of above-ground carbon depends upon vegetation densities, different vegetation indexes are used to calculate above-ground carbon storage [135,141–143]. However, Situmorang et al. [143] identified a strong positive correlation between the enhanced vegetation index (EVI) and above-ground carbon storage. Based on their findings, we have calculated above-ground carbon storage using the following Equation (4).

$$AGC = 151.7 \times EVI - 39.76 \quad (4)$$

where  $AGC$  is the above-ground carbon density and  $EVI$  is the enhanced vegetation index. The  $EVI$  was calculated using the Landsat 8 images based on Equation (5) [144].

$$EVI = 2.5 \times \frac{NIR - RED}{NIR + C1 \times RED - C2 \times BLUE + L} \quad (5)$$

where  $NIR$  is the near-infrared band,  $RED$  is the red band,  $BLUE$  is the blue band,  $C1$  is the values as coefficients for atmospheric resistance,  $C2$  is the values as coefficients for atmospheric resistance, and  $L$  is the value to adjust for the canopy background. In general, the values for  $C1$ ,  $C2$ , and  $L$  are 6, 7, and 1, respectively [145].

#### Standardization of Indicator Values

When employing the MCE option, the first and most important step is to transform each of the variables into factors. The difference between a variable and a factor is that a variable is unscaled with respect to the model, while a factor is scaled to a specific numeric range using a scaling procedure that is directly related to the expression of benefit or suitability [146]. For example, in the case of the  $ESV$ , a higher value of  $ESV$  would result in a higher environmental benefit, whereas a lower value of  $ESV$  would result in a lower environmental benefit. Therefore, the highest value would result in the maximum environmental benefit. The highest value can be given a value of 1, and the lowest value of

ESV can be assigned to 0. The values in between the highest and lowest values of ESV can be rescaled between 0 to 1. This rescaling is very important in multi-criteria evaluation. In the transition of multi-criteria evaluation, this process is known as standardization. Different methods are used for the standardization of variables. The most important methods include fuzzy, stepwise, max-min, and linear standardization [147]. However, the fuzzy membership function is a widely used method used in the standardization of variables in MCE. In this study, we used a fuzzy membership function for the standardization of the four variables.

### 3.4. Constructing the Environmental Benefits Index

Based on the values of all four indicators, finally, we have developed the composite index for the environmental benefits in urban land use allocation. To make a composite index, it is necessary to aggregate all the indicators. Different aggregation methods are available in the literature. Most of them include the ordered weighted averaging (OWA), artificial neural network (ANN), logic scoring of preference (LSP), and weighted linear combination (WLC) methods [148]. In this study, we used the OWA method to construct the EBI [149]. The OWA method was used in this study since OWA has the opportunity to adjust the level of risk in the multicriteria decision-making process. For example, in our case, if we want to protect an environmentally sensitive area (as determined by the environmental benefit) we may want to have low-risk, average-risk, and high-risk decisions available for decision-makers. However, the ANN, WLC, and LSP aggregation methods can generate only a single decision without alternatives, whereas the OWA method can generate a wide range of decision strategies for the decision-maker [149–152]. The OWA method uses a family of combination operators that allows for the continuous adjustment of both the risk and the tradeoff among the criteria, providing complete control in decision making. In the case of OWA, in addition to the criteria weight, a second set of weights known as ordered weights is applied to each factor [153]. Assigning a second weight to each criterion allows us to control the overall level of risk and tradeoff between the criteria to generate a wide range of decision outputs. In the OWA approach, the criteria values in a particular location (e.g., a single cell) are ordered from low to high. Then, ordered weights are assigned in either increasing order or decreasing order, considering the level of risk in the decision-making process. Detailed methods of OWA can be found elsewhere [149,150,153] and we are not going to describe the procedure in detail. The following OWA equation was used to derive the EBI:

$$EBI_i = \sum_{j=1}^n \left( \frac{u_j v_j}{\sum_{j=1}^n u_j v_j} \right) z_{ij} \quad (6)$$

where  $EBI_i$  is the environmental benefits index at the  $i$ th location,  $n$  is the number of indicators,  $u_j$  is the original weight factor of the criteria,  $v_j$  is the ordered weight of the criteria such that  $v_j \in [0, 1]$  for  $j = 1, 2, \dots, n$ , and  $\sum_{j=1}^n v_j = 1$ ,  $z_{ij}$  is the ordered value of the criteria at  $i$ th location.

In the case of OWA, two sets of weights are used. The first weight ( $u_j$ ) of the criteria can be determined using many methods, including the analytic network process (AHP) method [154], entropy method [155], and Delphi method [156], etc. Among others, the AHP method is the most popular and is used globally in the decision-making process. In this study, based on its popularity, we have used the AHP method to determine the weights of the indicators of environmental benefits in land use planning. A detailed method of calculating the weights of the indicators using the AHP method was described in our earlier study [157]. Therefore, we will not repeat the method here. The interested reader can see our earlier publication for more details. In this study, a focus group discussion was conducted with 15 professionals, including environmental experts, urban planners, and ecologists, to determine the weights of the indicators using the AHP method. After

calculating the weights, the consistency ratio was also calculated to check if there was consistency of judgment. The consistency ratio ( $CR$ ) was calculated using Equation (7).

$$CR = \frac{CI}{RI} \quad (7)$$

where,  $CI$  and  $RI$  represent the consistency index and random index, respectively, in which

$$CI = \frac{\lambda_{max} - n}{n - 1} \quad (8)$$

where,  $\lambda_{max}$  and  $n$  are the eigenvalue and the size of the matrix, respectively.

It is acceptable to have a consistency ratio of up to 10%, but minor variations are not a concern. Large deviations, on the other hand, suggest that the assessments are not perfect and need to be improved [158].

The second weight, which is known as the ordered weight, was assigned on the ordered criteria, either based on increasing order or decreasing order depending on the level of acceptable risk and the type of criteria. In our case, we are generating environmental benefit, so if we derive a high value of EBI, it will be low-risk and if we derive a low value of EBI, it will be a high-risk, considering the protection of the environmentally sensitive area. Therefore, we assigned ordered weights in the decreasing order (0.4, 0.3, 0.2, 0.1) to derive a low value of EBI (high-risk decision), and we also assigned ordered weights in increasing order (0.1, 0.2, 0.3, 0.4) to derive a high value of EBI (low-risk decision). It can be noted that we used four criteria to construct the EBI. Therefore, we used four ordered weights. It can also be noted that according to Equation (6), the sum of the ordered weights must be equal to 1 ( $\sum_{j=1}^n v_j = 1$ ). A set of equal ordered weights (0.25) was also assigned to each criterion to derive the average EBI value (average-risk decision). Thus, we generated three EBI scenarios in the study area with the low-risk decision, average-risk decision, and high-risk decision. After the calculation of the EBI value, we classified the EBI value into five levels. These levels were very low (0.00–0.20), low (0.20–0.40), medium (0.40–0.60), high (0.60–0.80), and very high (0.80–1.00).

## 4. Results and Discussion

### 4.1. Environmental Benefit Indicators

In Section 2, we elaborately discussed the different types of indicators used to measure environmental benefits from land use planning. Table 1 in Section 2 provides the initial list of indicators that can be used to measure environmental benefits. In Section 3.3.1, we also mentioned that the indicators were finalized based on expert opinion. Based on the literature review and expert opinion, we selected four indicators that can be used to measure environmental benefits in land use allocation and optimization problems. These four indicators are (a) spatial compactness, (b) land surface temperature, (c) ecosystem service value, and (d) carbon storage. In the next section, the values of these four indicators are presented.

### 4.2. Value of the Indicators

In this study, we identified four indicators to develop a composite index to measure environmental benefits in land use allocation and optimization problems. These indicators are spatial compactness, land surface temperature, ecosystem service value, and carbon storage. This section describes the findings of these indicators. Based on the methods described in Section 3.3.2, we computed the value of each indicator.

Figures 4 and 5 show the values of the four indicators used to construct the composite EBI. Figure 4 shows the actual values of the four indicators calculated using the methods described in Section 3.3.2. Figure 5 shows the standardized values of all indicators. The standardized values range from 0 to 1 and were calculated using the fuzzy membership function as described at the end of Section 3.3.2. The standardization of factors was conducted in such a way that a higher value indicates a higher environmental benefit, whereas

a lower value indicates a lower environmental benefit. Figures 4a and 5a illustrate the cell-wise value of spatial compactness for the study area. For Figure 4a, the value of spatial compactness ranges between 0 and 8, and for Figure 5a, the values range from 0 to 1. Some earlier studies used a 0-to-8 scale to indicate the value of spatial compactness [31,99,159]. However, we used a 0-to-1 scale to represent spatial compactness. A higher value of compactness indicates that the same land use types are closely grouped, whereas a lower value indicates that the same land uses are dispersed. From Figures 4a and 5a, it is seen that, in some locations, the value of spatial compactness is higher, and, in some locations, the value is lower. It is also evident from those figures that the value of compactness is higher in the locations where there is a higher number of same land uses, and the value of compactness is lower in the places where the number of same land use types is low. A similar nature was also identified in the compactness values in some other studies [2,27,28,99]. However, there is a difference in the representation in the value of compactness. We present compactness values on a scale from 0 to 1, while, in other studies, the compactness values were represented on a scale from 0 to 8. The main reason is that previous studies used various indicators separately to evaluate land use allocation, whereas we combined all four indicators to develop a composite index. Therefore, the standardization of indicators is required. We believe that the representation of the compactness value on a scale from 0 to 1 is more suitable compared to a scale from 0 to 8.

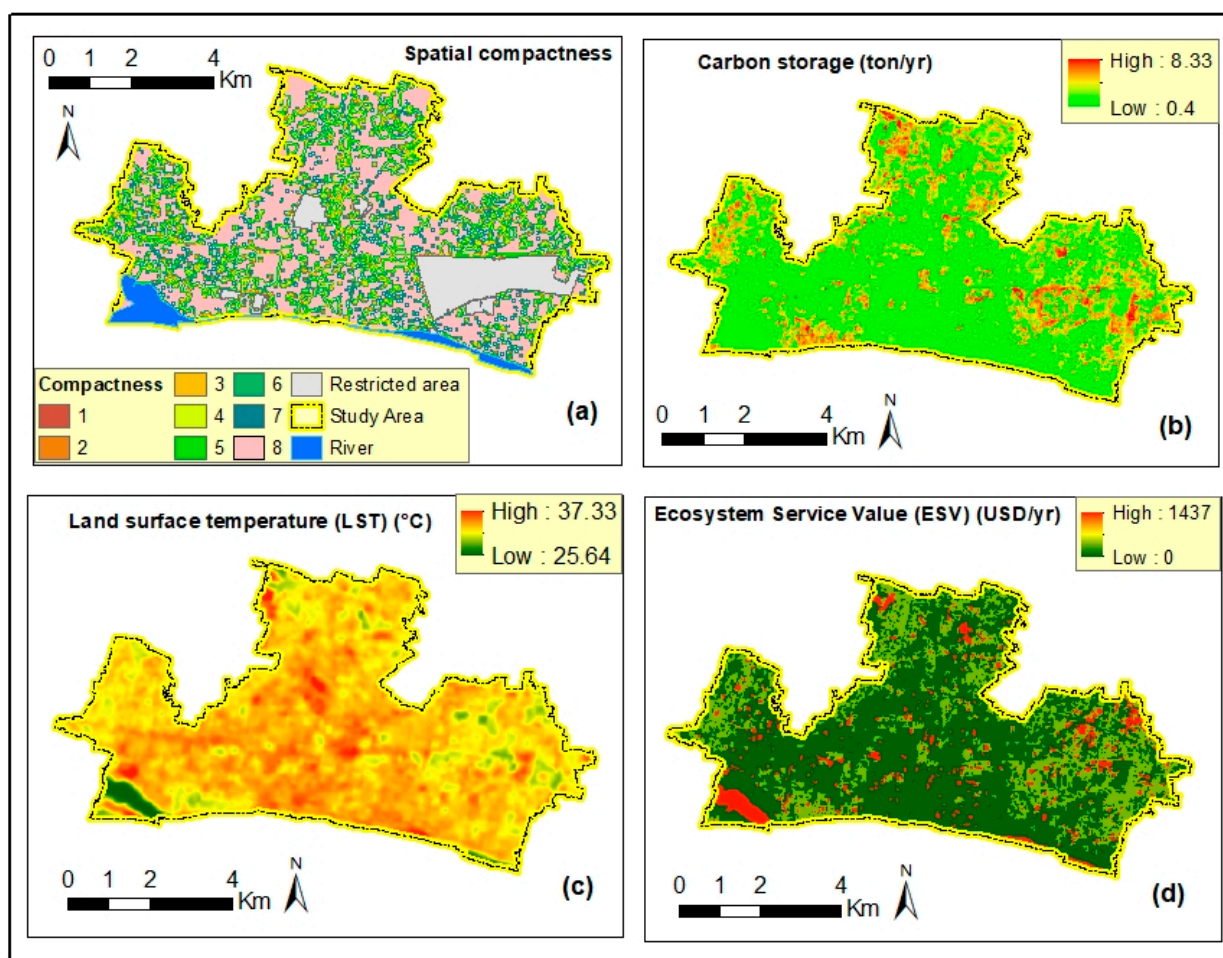


**Figure 4.** Original values of four indicators for the study area. (a) The spatial compactness in the top-left, (b) carbon storage in the top-right, (c) land surface temperature in the bottom-left, and (d) ecosystem service value in the bottom-right.

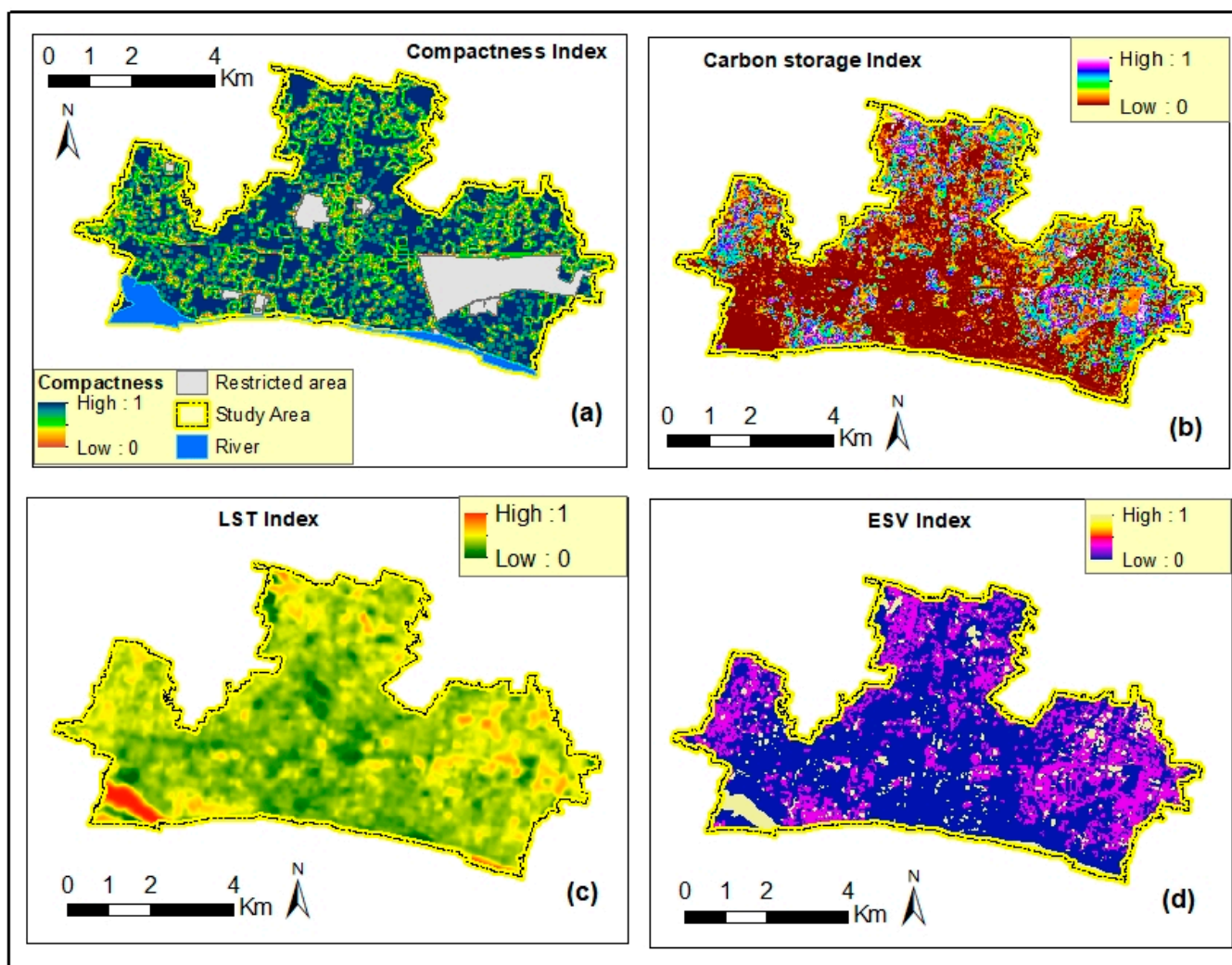


**Figure 5.** Standardized values of four indicators for the study area, as derived using the fuzzy membership function. (a) The spatial compactness index, (b) carbon storage index, (c) LST index, and (d) ecosystem service value index.

Figures 4b and 5b show the spatial distribution of carbon storage in the study area. As described in Section 3.3.2, carbon storage depends upon the density of vegetated carbon and soil organic carbon. Vegetated carbon was calculated based on the enhanced vegetation index (EVI), and SOC was calculated based on the density of SOC and the bulk density of soil. The spatial distribution of the EVI, vegetated carbon, and SOC are illustrated in Figure 6. Figure 6a illustrates that the value of the EVI in the study area ranges between  $-0.08$  and  $0.67$ .

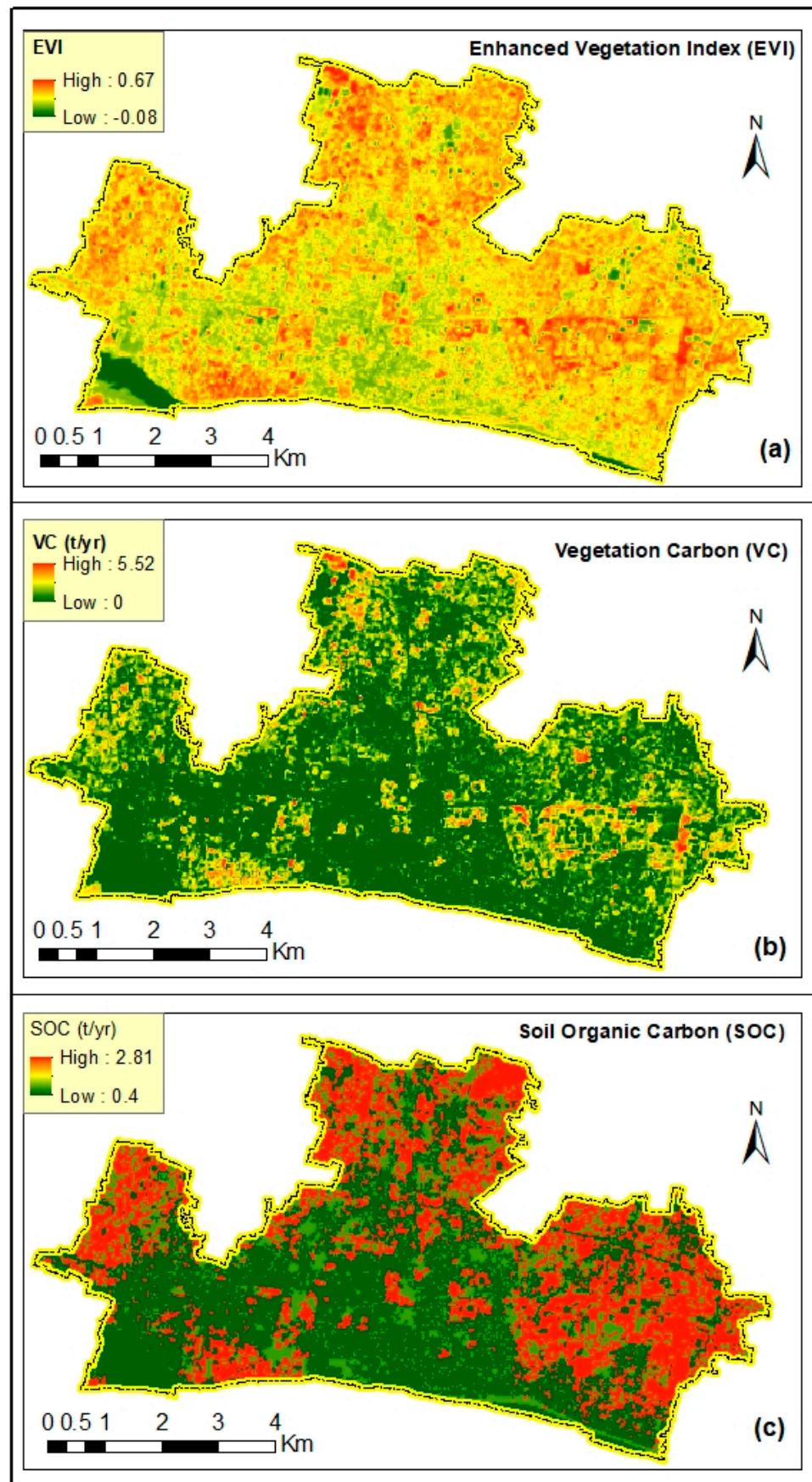


Figure 6. Map showing (a) the enhanced vegetation index, (b) vegetated carbon, and (c) soil organic carbon in the study area.

The EVI has a value range of  $-1$  to  $+1$ , and it ranges between  $0.2$  and  $0.8$  for healthy vegetation. A score nearer to  $1$  indicates healthy vegetation, whereas a value around  $-1$  indicates unhealthy vegetation [160]. The EVI was recently shown to be an effective approach for detecting vegetation changes and deriving the canopy biophysical features of a given location. The EVI is used to quantify the vegetation greenness of an area and for healthy vegetation. The EVI in the study area shows that the presence of healthy vegetation is low in the study area. However, the concentration of healthy vegetation is higher in the periphery compared to the central area. The total carbon storage in Figure 4b is the sum of the vegetated carbon and SOC in Figure 6b,c. According to Figure 4b, the minimum and maximum carbon storage per cell are  $0.4$  ton/year and  $8.33$  ton/year. The land cover type contributes to the value of carbon storage in the study area. In Figures 4b and 5b, we can see that the value of carbon storage is higher in the northern, southern, and eastern periphery of the study area, whereas the value of carbon storage is lower in the central part of the city. The reason is that the central part mainly comprises the built-up area with low vegetation cover. On the other hand, the northern, southern, and eastern periphery are characterized by a higher level of vegetation, agricultural land, and water bodies that contain high levels of carbon. Our findings are also supported by other studies where it is evident that vegetated land cover and agricultural land are associated with a high level of carbon storage, and that built-up areas are characterized by a low level of carbon storage [23,47,51,53,55].

The spatial distribution of LST is illustrated in Figures 4c and 5c. In Figure 4c, it is seen that the highest and lowest LST in the study area are  $37.33$  °C and  $25.64$  °C respectively. Urban land cover types play an important role in controlling LST, and LST affects human thermal comfort. Human thermal comfort (HTC) in urban areas informs city residents and planners about the negative effects on human health caused by excessive temperatures and a rise in LST [161]. Studies show that LST is associated with human thermal comfort. A higher LST in urban areas reduces human thermal comfort and has an impact on the urban environment and ecosystem [162]. Therefore, a higher value of LST indicates a lower level of environmental benefit, whereas a lower level of LST indicates higher environmental benefits. A value of LST ranging between  $21$  °C to  $24$  °C is considered to be a thermal comfort zone for humans [21]. From our study, it is evident that the LST in the entire study area is higher than the human thermal comfort range. In Figures 4c and 5c, it is observed that the central part of the city is characterized by higher temperatures compared to the periphery. The reason behind this variation is that the central part of the city is composed of more built-up areas, high population density, and transport activities, whereas the periphery is characterized by a higher level of vegetation and agriculture. Our study identifies that the LST is higher in built-up areas compared to vegetated land and agricultural land. Our finding is also supported by other studies [163–165].

The result of the ESV is illustrated in Figures 4d and 5d. The ESV was calculated based on the land cover map presented in Figure 7, Equation (2), and Table 4. Land cover is the primary data for the estimation of the ESV. Figure 7 shows the spatial distribution of land cover in the study area. According to Figure 7 and Table 6, built-up area is the most dominant land cover, which covers about  $34.95\%$  of the study area. The second dominant land cover type is vegetation ( $20.67\%$ ), followed by bare land ( $19.30\%$ ) and agriculture ( $17.11\%$ ). About  $7.98\%$  of the land belongs to water bodies. In Figure 7, it is observed that the central part and southern periphery are dominated by built-up areas, whereas the northern periphery is dominated by vegetation and agricultural land.

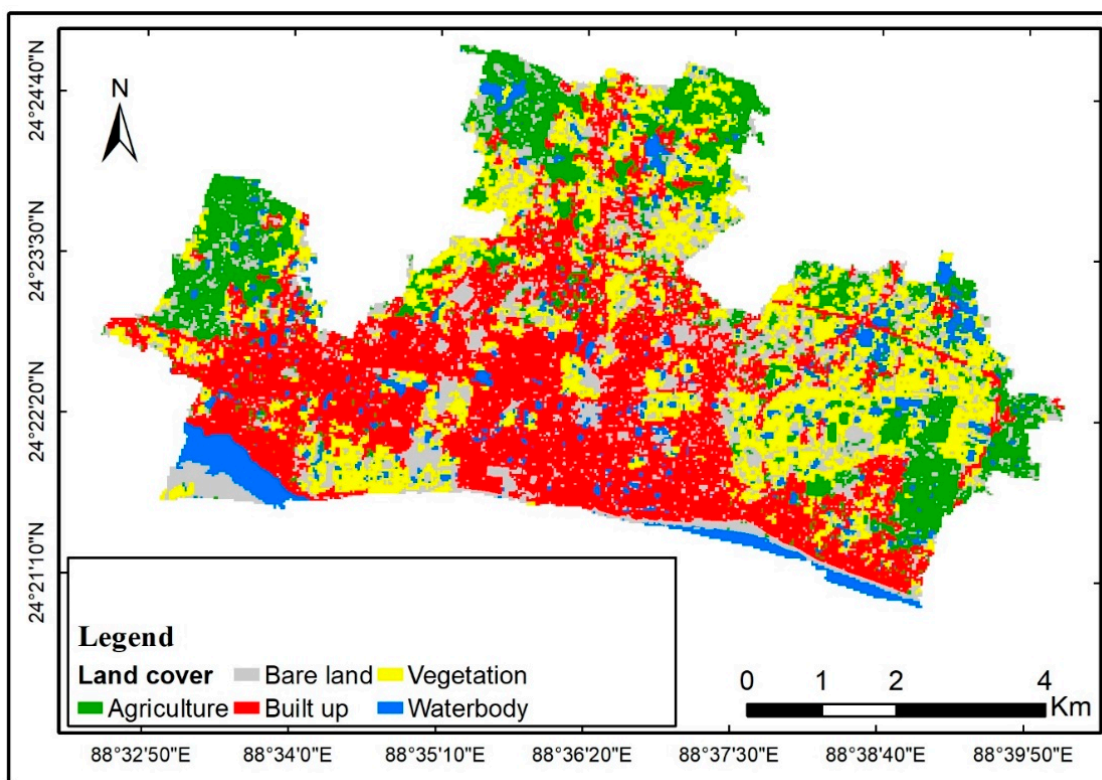


Figure 7. Land cover types in the study area.

Table 6. Different land cover types in the study area.

Land Cover	Area (SqKm)	Percentage
Agriculture	8.22	17.11
Bare land	9.28	19.30
Built-up	16.80	34.95
Vegetation	9.94	20.67
Waterbody	3.83	7.98
Total	48.07	100.00

Source: Author’s calculation.

The adjusted value coefficient for the year 2021 was used to calculate the ESV in the study area. In Figure 5d, it is seen that the maximum and minimum ESV in the study area were 1437 USD/year/cell and 0 USD/year/cell in the study area. A higher ESV results in a higher level of environmental benefit, whereas a lower ESV indicates a lower level of environmental benefit. The study finding shows that the ESV in the periphery is higher, and the ESV in the central city is close to 0. This means that the environmental benefit is higher in the periphery compared to the central part of the city. This spatial variation of ESV is also justified by the spatial distribution of land cover in the study area. As we can see from the land cover map in Figure 7, the built-up area is prevalent in the central part of the city, and the built-up area generates no ESV, according to Table 4; therefore, the ESV in the central part of the city is close to 0.

#### 4.3. Environmental Benefits Index (EBI) in the Study Area

Finally, Equation (6) and the weights of the indicators in Table 7 were used to determine the value of the EBI based on the value of four indicators. The AHP approach was used to calculate the weight of each indicator based on the experts’ judgment. Table 7 shows that the weight of spatial compactness, LST, carbon storage, and ESV were 0.1667, 0.4996, 0.0776, and 0.2562, respectively. The consistency ratio was 6%. As mentioned earlier, a consistency

ratio of less than 10% is acceptable. Therefore, the consistency ratio (6%) suggests that our weight determination using AHP is feasible. Table 7 shows that the LST is the most essential criterion in land use allocation for environmental benefit, whereas carbon storage has the least impact on environmental benefits. The importance of the LST in maintaining an urban environment was also highlighted in many studies [166,167]. The LST-induced urban heat island effect is becoming a global problem. Many studies have shown that the LST is an important factor in human comfort in urban areas [84].

**Table 7.** Weights of different indicators.

Indicators	Weight
Spatial compactness	0.1667
Land surface temperature	0.4996
Carbon storage	0.0776
Ecosystem service value	0.2562

Source: Author's calculation using the AHP method.

By using Equation (6) and weights from Table 7, we calculated the EBI for each cell in the study area with high-, low-, and average-risk decisions. The EBI's output is depicted in Figure 8. We categorized the EBI index into five tiers, as described at the end of Section 3.4. Table 8 shows the area under various EBI levels under different decision risk scenarios. Figure 8 shows the EBI in the study area at different levels of risk. Deriving alternative decision scenarios for the decision makers is common in many multi-criteria evaluations [150,151,153]. Figure 8a shows the EBI values in the study area with high-risk decisions. According to Figure 8a and Table 8, there would be no area with very high environmental benefits. Most of the area (48.31%) would fall within a low environmental benefit, followed by a very low environmental benefit (28.37%), and a medium level of environmental benefit (21.78%). Only 1.58% of land would fall within the high-level environmental benefit. Figure 8b illustrates the EBI values with the average-risk decision. According to Figure 8b and Table 8, the study area's minimum and maximum EBI values would range from 0.07 to 0.81. It is observed that, in an average-risk decision, no value greater than 0.8 would exist in the study area, except the river in the city's southwestern portion. This shows that the study area would not have a very high level of environmental benefit zone. It is also worth noting that only a small percentage of the land (3.83%) would have a high level of environmental value. About 95.56% of the land would have a very low to medium EBI value, with 2.54%, 64.55%, and 28.48% of land having very low, low, and medium EBI values, respectively. The medium EBI zone would encompass the majority of the land (64.55%). Figure 8c shows the EBI values in the study area with a low-risk decision. According to Figure 8c and Table 8, most of the area (50.88%) would fall within a medium environmental benefit, followed by a low environmental benefit (39.25%) and a high-level environmental benefit (8.00%). The three scenarios of the EBI have significance in decision making for the protection of environmentally sensitive areas. In a low-risk decision, the EBI is higher compared to average-risk and high-risk decisions. The decision maker will create more areas with high EBI values in the low-risk scenario to make decision making easier for the protection of environmentally sensitive areas.

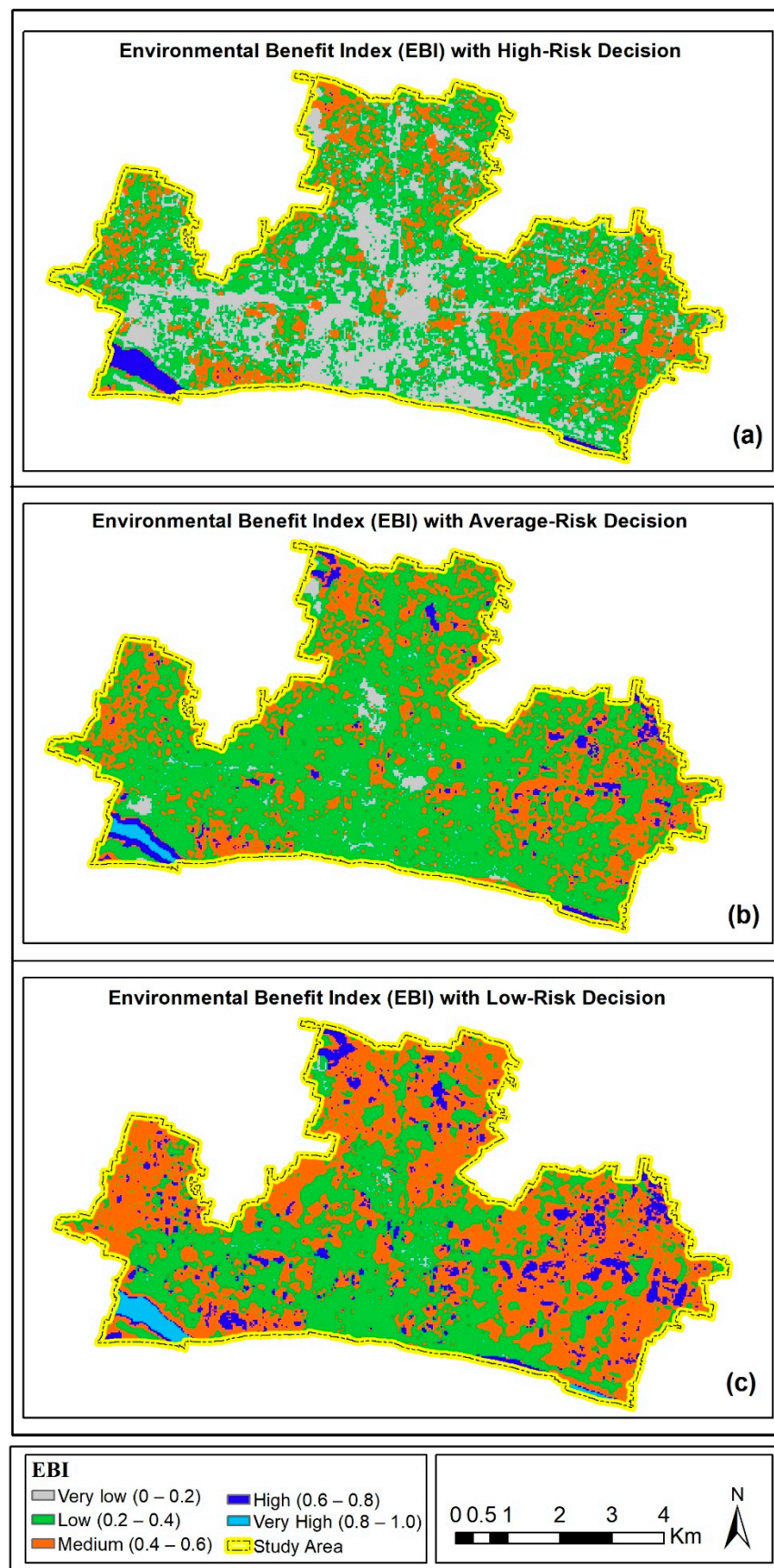


**Figure 8.** Level of environmental benefit in the study area with a (a) high-risk decision, (b) average-risk decision, and (c) low-risk decision.

We strongly argue that our proposed index is a much better approach compared to other measures of environmental benefits. Because, in previous studies, only one indicator was used to measure the environmental benefits. For example, spatial compactness, LST, carbon storage, and ESV were used separately to measure the environmental benefits. However, we contend that a single metric may not be the best way to assess environmental benefits. Rather, a composite index is necessary to better understand the environmental benefits in an urban area. In comparison, to separately assess environmental indicators, an environmental index provides several benefits. To begin, it is more easily interpretable and facilitates communication with environmental managers and the broader community. Additionally, it encourages accountability and results in similar long-term evaluations of an environmental system. Another issue with a single variable measure of environmental benefits is that the single variable may have disadvantages that could be overlooked. For example, according to Jenks and Jones [94], while urban spatial compactness has numerous environmental benefits, it can also result in reduced living space, less access to open spaces, less affordable housing, and worse health. Similarly, even a compact city may suffer negative consequences if the adjacent land uses are not compatible with each other. For example, if residential and industrial land coexists, it will create enormous problems for the people living near the industry. Likewise, if a city is spatially compact, as desired due to the benefits of a compact city, but the city lacks vegetated land cover, then there may be a high temperature, which may lead to human thermal discomfort. At the same time, insufficient vegetation and water bodies would result in a lower ESV, which is not good for the environmental quality and environmental sustainability of a city. Therefore, various factors, in combination, may play a role in the calculation of environmental benefits. Based on this idea, we proposed a composite index comprising spatial compactness, LST, carbon storage, and ESV. While there are some examples of environmental indices, those indices hardly focused on the sole urban area. Although there are some examples of multi-variable environmental measures, those did not only consider spatial variables relating to land use allocation. For example, the environmental performance index (EPI) is a composite indicator of overall environmentally sustainable development in a country. The index combines variables obtained from underlying sources to provide a composite picture of national environmental stewardship [168]. However, this index does not focus on urban-scale environmental benefits. Moreover, there are some indicators associated with the EPI that are not better understood in the context of land use allocation. For example, fisheries, sanitation, and drinking water were considered in developing the EPI, which are not associated with urban land use allocation. Široka et al. [169] developed a port environmental index (PEI) to measure the environmental quality in the seaport area. PEI was mainly concentrated on the pollution aspect of the environmental quality of a seaport. Zhou, Delmas and Kohli [170] developed a composite environmental index (CEI) to enable comparing the environmental performance among cities. However, they only considered toxin-related data to construct the CEI. Thus, it is evident that the proposed index will be the best approach compared to the single-indicator-based approach to describe the environmental benefits in urban land use allocation.

**Table 8.** The area under different EBI levels in the study area.

EBI Level	High-Risk Decision		Average-Risk Decision		Low-Risk Decision	
	Area (Sq.km)	%	Area (Sq.km)	%	Area (Sq.km)	%
Very low	13.64	28.37	1.219	2.54	0.16	0.34
Low	23.22	48.31	31.024	64.55	18.86	39.25
Medium	10.47	21.78	13.691	28.48	24.46	50.88
High	0.74	1.54	1.843	3.83	3.85	8.00
Very High	0	0	0.289	0.60	0.73	1.52
Total	48.065	100	48.065	100.00	48.065	100.00

Sources: Author's calculation based on the proposed EBI index.

In general, the study area is characterized by a low EBI. This lower EBI value indicates that the study area's land use allocation is not optimal. Rather, the city grew haphazardly. It is also worth noting that the majority of the city's periphery is classified as medium EBI, while the western side is characterized by extremely low and low EBI levels. The indicative value of EBI is also supported by the present land cover scenario in the study area. It is worth noting that the LST is the most significant contributor to the EBI. The LST is also affected by the kind of land cover. The LST is higher in urban areas and lowers in vegetated areas, water bodies, and agricultural areas. The EBI is higher in the periphery area because vegetated areas, aquatic bodies, and agricultural land predominate. The spatial distribution of the EBI over the territory indicates that the city's land use plan is inappropriate. This necessitates immediate intervention in the study area to improve land use planning.

We believe that the EBI value in this area is considerably lower due to unplanned growth in Rajshahi city. The unplanned growth was also recognized in the planning literature in the area. Unplanned development has been linked to a variety of factors. The city lacks a clear land use plan. The city's first master plan, which includes four hierarchical stages: a strategic plan, a structure plan, a functional master, and detailed area development plans, was completed in 2004 to guide the city's future development. There was no appropriate land use plan in this master plan, but the master plan was just an indicative plan without a proper guideline for land use development. At the same time, there was no effective development regulation or monitoring. As a result, the city was built chaotically. In addition to the lack of a formal land use plan, several hurdles prevented the city's physical expansion and development in a planned manner. In a nutshell, we can say the lower value of the EBI is the result of improper land use plans in the city.

## 5. Conclusions

Quantifying the environmental benefits in urban land use allocation is an important consideration to achieve urban sustainability and is of greater interest among researchers. However, there is limited research on this topic. This study developed a composite index based on four spatial indicators to measure environmental benefits in urban land use allocation. The main contribution and novelty of this paper are that previously a single indicator was used to measure environmental benefits in urban land use allocation, but this paper developed a composite index using multiple indicators. This study finds that the LST, spatial compactness, ESV, and carbon storage are the key indicators of environmental benefits in urban land use allocation, of which the LST is the most influential indicator of the EBI, while carbon storage has a low influence on the EBI. The result also suggests that the land use allocation in the study area is not optimal from an environmental point of view. It was also noticed that, with an average-risk decision, only a negligible portion of the city (3.83%) would fall within a high level of environmental benefit, while about 95.56% of the land would fall within a very low to medium EBI, of which the highest portion of land (64.55%) would fall within the medium EBI zone. The proposed environmental benefits index and the relevant analysis would help the decision-makers in many ways. The EBI values show the level of environmental benefits throughout the area. Therefore, the policy makers can take attention to the area where the EBI value is low. The policy makers can identify the reasons why the EBI is lower in a particular area and can take the necessary measures. This EBI would also help to devise appropriate policy interventions for increasing environmental benefits in the city. Although the proposed index is expected to offer a good way of measuring environmental benefits, there are also some limitations. Firstly, in this study, we considered the most appropriate four indicators to develop the composite index. However, the environmental benefits of land use allocation are very broad. Therefore, other indicators might have an impact on environmental benefits. Secondly, we used the OWA method to aggregate the indicators. However, there are also some other aggregation techniques, such as the Bonferroni method [171] and Choquet integral [172], that could generate new insights. Future research may be conducted to address these issues by adding more indicators and using different aggregation methods.

**Author Contributions:** Conceptualization, Md. Mostafizur Rahman; methodology, Md. Mostafizur Rahman; software, Md. Mostafizur Rahman; validation, Md. Mostafizur Rahman; formal analysis, Md. Mostafizur Rahman; investigation, Md. Mostafizur Rahman; resources, Md. Mostafizur Rahman; data curation, Md. Mostafizur Rahman; writing—original draft preparation, Md. Mostafizur Rahman; writing—review and editing, Md. Mostafizur Rahman and György Szabó; supervision, György Szabó. All authors have read and agreed to the published version of the manuscript.

**Funding:** This research received no external funding.

**Institutional Review Board Statement:** Not applicable.

**Informed Consent Statement:** Not applicable.

**Data Availability Statement:** The datasets used in this study are available from the corresponding author on request.

**Acknowledgments:** This research work is an output of a Doctoral study at the Department of Photogrammetry and Geoinformatics, Budapest University of Technology and Economics. The first author thanks the Ministry of Foreign Affairs and Trade and the Tempus Public Foundation of the Hungarian Government for providing the opportunity to study for a Ph.D. with the Stipendium Hungaricum Scholarship.

**Conflicts of Interest:** The authors declare no conflict of interest.

## References

1. Cao, K.; Batty, M.; Huang, B.; Liu, Y.; Yu, L.; Chen, J. Spatial multi-objective land use optimization: Extensions to the non-dominated sorting genetic algorithm-II. *Int. J. Geogr. Inf. Sci.* **2011**, *25*, 1949–1969. [[CrossRef](#)]
2. Sahebgharani, A. Multi-objective land use optimization through parallel particle swarm algorithm: Case study baboldasht district of isfahan, iran. *J. Urban Environ. Eng.* **2016**, *10*, 42–49. [[CrossRef](#)]
3. Lubida, A.; Veysipanah, M.; Pilesjo, P.; Mansourian, A. Land-use planning for sustainable urban development in Africa: A spatial and multi-objective optimization approach. *Geodesy Cartogr.* **2019**, *45*, 1–15. [[CrossRef](#)]
4. Rahman, M.; Szabó, G. Multi-objective urban land use optimization using spatial data: A systematic review. *Sustain. Cities Soc.* **2021**, *74*, 103214. [[CrossRef](#)]
5. Vardoulakis, S.; Dear, K.; Wilkinson, P. Challenges and Opportunities for Urban Environmental Health and Sustainability: The HEALTHY-POLIS initiative. *Environ. Health* **2016**, *15*, 1–4. [[CrossRef](#)] [[PubMed](#)]
6. Vardoulakis, S.; Kinney, P. Grand Challenges in Sustainable Cities and Health. *Front. Sustain. Cities* **2019**, *1*, 7. [[CrossRef](#)]
7. Koop, S.H.A.; Van Leeuwen, C.J. The challenges of water, waste and climate change in cities. *Environ. Dev. Sustain.* **2017**, *19*, 385–418. [[CrossRef](#)]
8. Deng, X.; Huang, J.; Rozelle, S.; Zhang, J.; Li, Z. Impact of urbanization on cultivated land changes in China. *Land Use Policy* **2015**, *45*, 1–7. [[CrossRef](#)]
9. Atasoy, M. Assessing the impacts of land-use/land-cover change on the development of urban heat island effects. *Environ. Dev. Sustain.* **2019**, *22*, 7547–7557. [[CrossRef](#)]
10. Kuo, H.-F.; Tsou, K.-W. Modeling and Simulation of the Future Impacts of Urban Land Use Change on the Natural Environment by SLEUTH and Cluster Analysis. *Sustainability* **2018**, *10*, 72. [[CrossRef](#)]
11. Liu, F.; Zhang, X.; Murayama, Y.; Morimoto, T. Impacts of Land Cover/Use on the Urban Thermal Environment: A Comparative Study of 10 Megacities in China. *Remote Sens.* **2020**, *12*, 307. [[CrossRef](#)]
12. Javanbakht, M.; Bolorani, A.D.; Kiavarz, M.; Samany, N.N.; Zebardast, L.; Zangiabadi, M. Spatial-temporal analysis of urban environmental quality of Tehran, Iran. *Ecol. Indic.* **2021**, *120*, 106901. [[CrossRef](#)]
13. Hsueh, S.L.; Lin, Y.J. Critical success factors of the urban environmental quality. *Ekoloji* **2018**, *27*, 217–222.
14. Mishra, H.S.; Bell, S.; Vassiljev, P.; Kuhlmann, F.; Niin, G.; Grellier, J. The development of a tool for assessing the environmental qualities of urban blue spaces. *Urban For. Urban Green.* **2020**, *49*, 126575. [[CrossRef](#)]
15. Caprotti, F. Critical research on eco-cities? A walk through the Sino-Singapore Tianjin Eco-City, China. *Cities* **2014**, *36*, 10–17. [[CrossRef](#)]
16. Yu, L. Low carbon eco-city: New approach for Chinese urbanisation. *Habitat Int.* **2014**, *44*, 102–110. [[CrossRef](#)]
17. Yuan, M.; Liu, Y.; He, J.; Liu, D. Regional land-use allocation using a coupled MAS and GA model: From local simulation to global optimization, a case study in Caidian District, Wuhan, China. *Cartogr. Geogr. Inf. Sci.* **2014**, *41*, 363–378. [[CrossRef](#)]
18. Mouratidis, K. Is compact city livable? The impact of compact versus sprawled neighbourhoods on neighbourhood satisfaction. *Urban Stud.* **2018**, *55*, 2408–2430. [[CrossRef](#)]
19. Kotulla, T.; Denstadli, J.M.; Oust, A.; Beusker, E. What Does It Take to Make the Compact City Liveable for Wider Groups? Identifying Key Neighbourhood and Dwelling Features. *Sustainability* **2019**, *11*, 3480. [[CrossRef](#)]
20. Nadeem, M.; Aziz, A.; Al-Rashid, M.A.; Tesoriere, G.; Asim, M.; Campisi, T. Scaling the Potential of Compact City Development: The Case of Lahore, Pakistan. *Sustainability* **2021**, *13*, 5257. [[CrossRef](#)]

21. Giannaros, T.M.; Melas, D.; Daglis, I.A.; Keramitsoglou, I. Development of an operational modeling system for urban heat islands: An application to Athens, Greece. *Nat. Hazards Earth Syst. Sci.* **2014**, *14*, 347–358. [[CrossRef](#)]
22. Keith, H.; Vardon, M.; Stein, J.; Lindenmayer, D. Contribution of native forests to climate change mitigation—A common approach to carbon accounting that aligns results from environmental-economic accounting with rules for emissions reduction. *Environ. Sci. Policy* **2019**, *93*, 189–199. [[CrossRef](#)]
23. Zarandian, A.; Badamfirouz, J.; Musazadeh, R.; Rahmati, A.; Azimi, S.B. Scenario modeling for spatial-temporal change detection of carbon storage and sequestration in a forested landscape in Northern Iran. *Environ. Monit. Assess.* **2018**, *190*, 474. [[CrossRef](#)]
24. Zinia, N.J.; McShane, P. Urban ecosystems and ecosystem services in megacity Dhaka: Mapping and inventory analysis. *Urban Ecosyst.* **2021**, *24*, 915–928. [[CrossRef](#)]
25. Zank, B.; Bagstad, K.J.; Voigt, B.; Villa, F. Modeling the effects of urban expansion on natural capital stocks and ecosystem service flows: A case study in the Puget Sound, Washington, USA. *Landsc. Urban Plan.* **2016**, *149*, 31–42. [[CrossRef](#)]
26. Mouratidis, K. Compact city, urban sprawl, and subjective well-being. *Cities* **2019**, *92*, 261–272. [[CrossRef](#)]
27. Yang, L.; Sun, X.; Peng, L.; Shao, J.; Chi, T. An improved artificial bee colony algorithm for optimal land-use allocation. *Int. J. Geogr. Inf. Sci.* **2015**, *29*, 1470–1489. [[CrossRef](#)]
28. Liu, Y.; Tang, W.; He, J.; Liu, Y.; Ai, T.; Liu, D. A land-use spatial optimization model based on genetic optimization and game theory. *Comput. Environ. Urban Syst.* **2015**, *49*, 1–14. [[CrossRef](#)]
29. Schwaab, J.; Deb, K.; Goodman, E.; Lautenbach, S.; van Strien, M.J.; Grêt-Regamey, A. Improving the performance of genetic algorithms for land-use allocation problems. *Int. J. Geogr. Inf. Sci.* **2018**, *32*, 907–930. [[CrossRef](#)]
30. Handayanto, R.T.; Tripathi, N.K.; Kim, S.M.; Guha, S. Achieving a Sustainable Urban Form through Land Use Optimisation: Insights from Bekasi City’s Land-Use Plan (2010–2030). *Sustainability* **2017**, *9*, 221. [[CrossRef](#)]
31. Li, F.; Gong, Y.; Cai, L.; Sun, C.; Chen, Y.; Liu, Y.; Jiang, P. Sustainable Land-Use Allocation: A Multiobjective Particle Swarm Optimization Model and Application in Changzhou, China. *J. Urban Plan. Dev.* **2018**, *144*, 04018010. [[CrossRef](#)]
32. Park, C.; Ha, J.; Lee, S. Association between Three-Dimensional Built Environment and Urban Air Temperature: Seasonal and Temporal Differences. *Sustainability* **2017**, *9*, 1338. [[CrossRef](#)]
33. Choi, Y.; Lee, S.; Moon, H. Urban Physical Environments and the Duration of High Air Temperature: Focusing on Solar Radiation Trapping Effects. *Sustainability* **2018**, *10*, 4837. [[CrossRef](#)]
34. Zhao, Q.; Myint, S.W.; Wentz, E.A.; Fan, C. Rooftop Surface Temperature Analysis in an Urban Residential Environment. *Remote Sens.* **2015**, *7*, 12135–12159. [[CrossRef](#)]
35. Lee, S.; Ha, J.; Cho, H. Spatial and Temporal Effects of Built Environment on Urban Air Temperature in Seoul City, Korea: An Application of Spatial Regression Models. *J. Asian Arch. Build. Eng.* **2017**, *16*, 123–130. [[CrossRef](#)]
36. Pu, R. Assessing scaling effect in downscaling land surface temperature in a heterogenous urban environment. *Int. J. Appl. Earth Obs. Geoinf.* **2021**, *96*, 102256. [[CrossRef](#)]
37. Baró, F.; Chaparro, L.; Gómez-Baggethun, E.; Langemeyer, J.; Nowak, D.J.; Terradas, J. Contribution of Ecosystem Services to Air Quality and Climate Change Mitigation Policies: The Case of Urban Forests in Barcelona, Spain. *Ambio* **2014**, *43*, 466–479. [[CrossRef](#)]
38. Agathangelidis, I.; Cartalis, C. Improving the disaggregation of MODIS land surface temperatures in an urban environment: A statistical downscaling approach using high-resolution emissivity. *Int. J. Remote Sens.* **2019**, *40*, 5261–5286. [[CrossRef](#)]
39. Wang, Z.; Cao, J.; Zhu, C.; Yang, H. The Impact of Land Use Change on Ecosystem Service Value in the Upstream of Xiong’an New Area. *Sustainability* **2020**, *12*, 5707. [[CrossRef](#)]
40. Grafius, D.R.; Corstanje, R.; Warren, P.H.; Evans, K.L.; Hancock, S.; Harris, J.A. The impact of land use/land cover scale on modelling urban ecosystem services. *Landsc. Ecol.* **2016**, *31*, 1509–1522. [[CrossRef](#)]
41. Lin, X.; Xu, M.; Cao, C.; Singh, R.P.; Chen, W.; Ju, H. Land-Use/Land-Cover Changes and Their Influence on the Ecosystem in Chengdu City, China during the Period of 1992–2018. *Sustainability* **2018**, *10*, 3580. [[CrossRef](#)]
42. Sharma, R.; Rimal, B.; Baral, H.; Nehren, U.; Paudyal, K.; Sharma, S.; Rijal, S.; Ranpal, S.; Acharya, R.P.; Alenazy, A.A.; et al. Impact of Land Cover Change on Ecosystem Services in a Tropical Forested Landscape. *Resources* **2019**, *8*, 18. [[CrossRef](#)]
43. Arunyawat, S.; Shrestha, R.P. Assessing Land Use Change and Its Impact on Ecosystem Services in Northern Thailand. *Sustainability* **2016**, *8*, 768. [[CrossRef](#)]
44. Wang, Z.; Zhang, B.; Zhang, S.; Li, X.; Liu, D.; Song, K.; Li, J.; Li, F.; Duan, H. Changes of Land Use and of Ecosystem Service Values in Sanjiang Plain, Northeast China. *Environ. Monit. Assess.* **2006**, *112*, 69–91. [[CrossRef](#)]
45. Tolessa, T.; Senbeta, F.; Kidane, M. The impact of land use/land cover change on ecosystem services in the central highlands of Ethiopia. *Ecosyst. Serv.* **2017**, *23*, 47–54. [[CrossRef](#)]
46. Quintas-Soriano, C.; Castro, A.J.; Castro, H.; García-Llorente, M. Impacts of land use change on ecosystem services and implications for human well-being in Spanish drylands. *Land Use Policy* **2016**, *54*, 534–548. [[CrossRef](#)]
47. Chen, Y.; Lu, H.; Li, J.; Xia, J. Effects of land use cover change on carbon emissions and ecosystem services in Chengyu urban agglomeration, China. *Stoch. Hydrol. Hydraul.* **2020**, *34*, 1197–1215. [[CrossRef](#)]
48. Yang, Q.; Mašek, O.; Zhao, L.; Nan, H.; Yu, S.; Yin, J.; Li, Z.; Cao, X. Country-level potential of carbon sequestration and environmental benefits by utilizing crop residues for biochar implementation. *Appl. Energy* **2021**, *282*, 116275. [[CrossRef](#)]
49. Zhao, C.; Sander, H.A. Quantifying and Mapping the Supply of and Demand for Carbon Storage and Sequestration Service from Urban Trees. *PLoS ONE* **2015**, *10*, e0136392. [[CrossRef](#)] [[PubMed](#)]

50. Arehart, J.H.; Nelson, W.S.; Srubar, W.V. On the theoretical carbon storage and carbon sequestration potential of hempcrete. *J. Clean. Prod.* **2020**, *266*, 121846. [[CrossRef](#)]
51. Estrada, G.C.D.; Soares, M.L.G.; Fernandez, V.; De Almeida, P.M.M. The economic evaluation of carbon storage and sequestration as ecosystem services of mangroves: A case study from southeastern Brazil. *Int. J. Biodivers. Sci. Ecosyst. Serv. Manag.* **2014**, *11*, 29–35. [[CrossRef](#)]
52. Ma, J.; Li, X.; Baoquan, J.; Liu, X.; Li, T.; Zhang, W.; Liu, W. Spatial variation analysis of urban forest vegetation carbon storage and sequestration in built-up areas of Beijing based on i-Tree Eco and Kriging. *Urban For. Urban Green.* **2021**, *66*, 127413. [[CrossRef](#)]
53. Russo, A.; Escobedo, F.J.; Timilsina, N.; Schmitt, A.O.; Varela, S.; Zerbe, S. Assessing urban tree carbon storage and sequestration in Bolzano, Italy. *Int. J. Biodivers. Sci. Ecosyst. Serv. Manag.* **2014**, *10*, 54–70. [[CrossRef](#)]
54. Nowak, D.J.; Greenfield, E.J.; Hoehn, R.E.; Lapoint, E. Carbon storage and sequestration by trees in urban and community areas of the United States. *Environ. Pollut.* **2013**, *178*, 229–236. [[CrossRef](#)]
55. Pache, R.-G.; Abrudan, I.V.; Niță, M.-D. Economic Valuation of Carbon Storage and Sequestration in Retezat National Park, Romania. *Forests* **2021**, *12*, 43. [[CrossRef](#)]
56. Adelisardou, F.; Zhao, W.; Chow, R.; Mederly, P.; Minkina, T.; Schou, J.S. Spatiotemporal change detection of carbon storage and sequestration in an arid ecosystem by integrating Google Earth Engine and InVEST (the Jiroft plain, Iran). *Int. J. Environ. Sci. Technol.* **2021**, 1–16. [[CrossRef](#)]
57. Shekarrizfard, M.; Imani, A.F.; Crouse, D.L.; Goldberg, M.; Ross, N.; Eluru, N.; Hatzopoulou, M. Individual exposure to traffic related air pollution across land-use clusters. *Transp. Res. Part D Transp. Environ.* **2016**, *46*, 339–350. [[CrossRef](#)]
58. Krupnova, T.G.; Rakova, O.V.; Plaksina, A.L.; Gavrilkina, S.V.; Baranov, E.O.; Abramyana, A.D. Short Communication: Effect of urban greening and land use on air pollution in Chelyabinsk, Russia. *Biodiversitas J. Biol. Divers.* **2020**, *21*. [[CrossRef](#)]
59. Liu, H.; Weng, Q. Scaling Effect of Fused ASTER-MODIS Land Surface Temperature in an Urban Environment. *Sensors* **2018**, *18*, 4058. [[CrossRef](#)]
60. Khomenko, S.; Cirach, M.; Pereira-Barboza, E.; Mueller, N.; Barrera-Gómez, J.; Rojas-Rueda, D.; de Hoogh, K.; Hoek, G.; Nieuwenhuijsen, M. Premature mortality due to air pollution in European cities: A health impact assessment. *Lancet Planet. Health* **2021**, *5*, e121–e134. [[CrossRef](#)]
61. Han, L.; Zhou, W.; Pickett, S.T.; Li, W.; Qian, Y. Multicontaminant air pollution in Chinese cities. *Bull. World Health Organ.* **2018**, *96*, 233–242E. [[CrossRef](#)]
62. Kumar, P.; Morawska, L.; Martani, C.; Biskos, G.; Neophytou, M.K.-A.; DI Sabatino, S.; Bell, M.; Norford, L.; Britter, R. The rise of low-cost sensing for managing air pollution in cities. *Environ. Int.* **2015**, *75*, 199–205. [[CrossRef](#)]
63. Wei, G.; Zhang, Z.; Ouyang, X.; Shen, Y.; Jiang, S.; Liu, B.; He, B.-J. Delineating the spatial-temporal variation of air pollution with urbanization in the Belt and Road Initiative area. *Environ. Impact Assess. Rev.* **2021**, *91*, 106646. [[CrossRef](#)]
64. Luo, H.; Guan, Q.; Lin, J.; Wang, Q.; Yang, L.; Tan, Z.; Wang, N. Air pollution characteristics and human health risks in key cities of northwest China. *J. Environ. Manag.* **2020**, *269*, 110791. [[CrossRef](#)] [[PubMed](#)]
65. Hoffmann, B. Air Pollution in Cities: Urban and Transport Planning Determinants and Health in Cities. In *Integrating Human Health into Urban and Transport Planning*; Springer: Cham, Switzerland, 2018; pp. 425–441. [[CrossRef](#)]
66. Sen, S.; Samuel, C.; Ajith, L. Pollution characteristics of soils and sediments of thoothukudi city. *Int. J. Eng. Adv. Technol.* **2019**, *8*, 697–702.
67. Pan, L.; Wang, Y.; Ma, J.; Hu, Y.; Su, B.; Fang, G.; Wang, L.; Xiang, B. A review of heavy metal pollution levels and health risk assessment of urban soils in Chinese cities. *Environ. Sci. Pollut. Res.* **2018**, *25*, 1055–1069. [[CrossRef](#)]
68. Fei, X.; Christakos, G.; Xiao, R.; Ren, Z.; Liu, Y.; Lv, X. Improved heavy metal mapping and pollution source apportionment in Shanghai City soils using auxiliary information. *Sci. Total Environ.* **2019**, *661*, 168–177. [[CrossRef](#)] [[PubMed](#)]
69. Polyakov, V.; Kozlov, A.; Suleymanov, A.; Abakumov, E. Soil pollution status of urban soils in St. Petersburg city, North-west of Russia. *Soil Water Res.* **2021**, *16*, 164–173. [[CrossRef](#)]
70. Yan, D.; Bai, Z.; Liu, X. Heavy-Metal Pollution Characteristics and Influencing Factors in Agricultural Soils: Evidence from Shuozhou City, Shanxi Province, China. *Sustainability* **2020**, *12*, 1907. [[CrossRef](#)]
71. Kharytonov, M.M.; Stankevich, S.; Titarenko, O.; Weissmannová, H.D.; Klimkina, I.I.; Frolova, L.A. Geostatistical and geospatial assessment of soil pollution with heavy metals in Pavlograd city (Ukraine). *Ecol. Quest.* **2020**, *31*, 1–20. [[CrossRef](#)]
72. Hu, B.; Shao, S.; Ni, H.; Fu, Z.; Huang, M.; Chen, Q.; Shi, Z. Assessment of potentially toxic element pollution in soils and related health risks in 271 cities across China. *Environ. Pollut.* **2021**, *270*, 116196. [[CrossRef](#)] [[PubMed](#)]
73. Adimalla, N. Heavy metals pollution assessment and its associated human health risk evaluation of urban soils from Indian cities: A review. *Environ. Geochem. Health* **2020**, *42*, 173–190. [[CrossRef](#)] [[PubMed](#)]
74. Zhang, X.; Zha, T.; Guo, X.; Meng, G.; Zhou, J. Spatial distribution of metal pollution of soils of Chinese provincial capital cities. *Sci. Total Environ.* **2018**, *643*, 1502–1513. [[CrossRef](#)]
75. Martin, M.; Poulidikou, S.; Molin, E. Exploring the Environmental Performance of Urban Symbiosis for Vertical Hydroponic Farming. *Sustainability* **2019**, *11*, 6724. [[CrossRef](#)]
76. Benis, K.; Ferrao, P. Commercial farming within the urban built environment—Taking stock of an evolving field in northern countries. *Glob. Food Secur.* **2018**, *17*, 30–37. [[CrossRef](#)]
77. Martin, M.; Molin, E. Environmental Assessment of an Urban Vertical Hydroponic Farming System in Sweden. *Sustainability* **2019**, *11*, 4124. [[CrossRef](#)]

78. Langendahl, P.-A. The Politics of Smart Farming Expectations in Urban Environments. *Front. Sustain. Cities* **2021**, *3*, 691951. [[CrossRef](#)]
79. Zhang, G.; He, B.-J. Towards green roof implementation: Drivers, motivations, barriers and recommendations. *Urban For. Urban Green.* **2021**, *58*, 126992. [[CrossRef](#)]
80. Zhao, D.; Arshad, M.; Wang, J.; Triantafilis, J. Soil exchangeable cations estimation using Vis-NIR spectroscopy in different depths: Effects of multiple calibration models and spiking. *Comput. Electron. Agric.* **2021**, *182*, 105990. [[CrossRef](#)]
81. Zhao, D.; Zhao, X.; Khongnawang, T.; Arshad, M.; Triantafilis, J. A Vis-NIR Spectral Library to Predict Clay in Australian Cotton Growing Soil. *Soil Sci. Soc. Am. J.* **2018**, *82*, 1347–1357. [[CrossRef](#)]
82. Mathew, A.; Khandelwal, S.; Kaul, N. Analysis of diurnal surface temperature variations for the assessment of surface urban heat island effect over Indian cities. *Energy Build.* **2018**, *159*, 271–295. [[CrossRef](#)]
83. Li, Y.; Sun, Y.; Li, J.; Gao, C. Socioeconomic drivers of urban heat island effect: Empirical evidence from major Chinese cities. *Sustain. Cities Soc.* **2020**, *63*, 102425. [[CrossRef](#)]
84. Chen, M.; Zhou, Y.; Hu, M.; Zhou, Y. Influence of Urban Scale and Urban Expansion on the Urban Heat Island Effect in Metropolitan Areas: Case Study of Beijing–Tianjin–Hebei Urban Agglomeration. *Remote Sens.* **2020**, *12*, 3491. [[CrossRef](#)]
85. Soltani, A.; Sharifi, E. Daily variation of urban heat island effect and its correlations to urban greenery: A case study of Adelaide. *Front. Arch. Res.* **2017**, *6*, 529–538. [[CrossRef](#)]
86. Yang, J.; Wang, Y.; Xue, B.; Li, Y.; Xiao, X.; Xia, J.; He, B. Contribution of urban ventilation to the thermal environment and urban energy demand: Different climate background perspectives. *Sci. Total. Environ.* **2021**, *795*, 148791. [[CrossRef](#)]
87. Luo, X.; Yang, J.; Sun, W.; He, B. Suitability of human settlements in mountainous areas from the perspective of ventilation: A case study of the main urban area of Chongqing. *J. Clean. Prod.* **2021**, *310*, 127467. [[CrossRef](#)]
88. Alexander, K.; Hettiarachchi, S.; Ou, Y.; Sharma, A. Can integrated green spaces and storage facilities absorb the increased risk of flooding due to climate change in developed urban environments? *J. Hydrol.* **2019**, *579*, 124201. [[CrossRef](#)]
89. Sjöman, H.; Levinsson, A.; Emilsson, T.; Ibrahimova, A.; Alizade, V.; Douglas, P.; Wiström, B. Evaluation of *Alnus* subcordata for urban environments through assessment of drought and flooding tolerance. *Dendrobiology* **2021**, *85*, 39–50. [[CrossRef](#)]
90. Akeh, G.I. Climate Change and Urban Flooding: Implications for Nigeria’s Built Environment. *MOJ Ecol. Environ. Sci.* **2016**, *1*, 1–4. [[CrossRef](#)]
91. Song, J.; Li, W. Linkage Between the Environment and Individual Resilience to Urban Flooding: A Case Study of Shenzhen, China. *Int. J. Environ. Res. Public Health* **2019**, *16*, 2559. [[CrossRef](#)]
92. Devi, N.N.; Sridharan, B.; Bindhu, V.M.; Narasimhan, B.; Bhallamudi, S.M.; Bhatt, C.M.; Usha, T.; Vasan, D.T.; Kuiry, S.N. Investigation of Role of Retention Storage in Tanks (Small Water Bodies) on Future Urban Flooding: A Case Study of Chennai City, India. *Water* **2020**, *12*, 2875. [[CrossRef](#)]
93. Avashia, V.; Garg, A. Implications of land use transitions and climate change on local flooding in urban areas: An assessment of 42 Indian cities. *Land Use Policy* **2020**, *95*, 104571. [[CrossRef](#)]
94. Jenks, M.; Jones, C. Issues and concepts. In *Dimensions of the Sustainable City*; Springer: Dordrecht, The Netherlands, 2010; pp. 1–19. [[CrossRef](#)]
95. Batten, D.C. The perils of urban consolidation: A discussion of Australian housing and urban development policies-Troy, PN’. *Urban Stud.* **1997**, *34*, 1915–1917.
96. Burton, E. The Compact City: Just or Just Compact? A Preliminary Analysis. *Urban Stud.* **2000**, *37*, 1969–2006. [[CrossRef](#)]
97. Kai, C.L.; Bo, H. Comparison of spatial compactness evaluation methods for simple genetic algorithm based land use planning optimization problem. In *International Archives of the Photogrammetry, Remote Sensing and Spatial Information Sciences*; ISPRS Archives; ISPRS Technical Commission II: Hong Kong, China, 2010.
98. Cao, K.; Huang, B.; Wang, S.; Lin, H. Sustainable land use optimization using Boundary-based Fast Genetic Algorithm. *Comput. Environ. Urban Syst.* **2012**, *36*, 257–269. [[CrossRef](#)]
99. Song, M.; Chen, D. An improved knowledge-informed NSGA-II for multi-objective land allocation (MOLA). *Geo Spat. Inf. Sci.* **2018**, *21*, 273–287. [[CrossRef](#)]
100. Song, M.; Chen, D. A comparison of three heuristic optimization algorithms for solving the multi-objective land allocation (MOLA) problem. *Ann. GIS* **2018**, *24*, 19–31. [[CrossRef](#)]
101. Aerts, J.C.J.H.; Eisinger, E.; Heuvelink, G.B.M.; Stewart, T.J. Using Linear Integer Programming for Multi-Site Land-Use Allocation. *Geogr. Anal.* **2003**, *35*, 148–169. [[CrossRef](#)]
102. Stewart, T.J.; Janssen, R.; van Herwijnen, M. A genetic algorithm approach to multiobjective land use planning. *Comput. Oper. Res.* **2004**, *31*, 2293–2313. [[CrossRef](#)]
103. Williams, J.C.; ReVelle, C.S. Reserve assemblage of critical areas: A zero-one programming approach. *Eur. J. Oper. Res.* **1998**, *104*, 497–509. [[CrossRef](#)]
104. Hu, Y. Batunacun an Analysis of Land-Use and Land-Cover Change in the Zhujiang–Xijiang Economic Belt, China, from 1990 to 2017. *Appl. Sci.* **2018**, *8*, 1524. [[CrossRef](#)]
105. González, J.E.; Ramamurthy, P.; Bornstein, R.D.; Chen, F.; Bou-Zeid, E.R.; Ghandehari, M.; Luvall, J.; Mitra, C.; Niyogi, D. Urban climate and resiliency: A synthesis report of state of the art and future research directions. *Urban Clim.* **2021**, *38*, 100858. [[CrossRef](#)]
106. Masson, V.; Lemonsu, A.; Hidalgo, J.; Voogt, J. Urban Climates and Climate Change. *Annu. Rev. Environ. Resour.* **2020**, *45*, 411–444. [[CrossRef](#)]

107. Choudhury, D.; Das, K.; Das, A. Assessment of land use land cover changes and its impact on variations of land surface temperature in Asansol-Durgapur Development Region. *Egypt. J. Remote Sens. Space Sci.* **2019**, *22*, 203–218. [[CrossRef](#)]
108. Zhang, Y.; Sun, L. Spatial-temporal impacts of urban land use land cover on land surface temperature: Case studies of two Canadian urban areas. *Int. J. Appl. Earth Obs. Geoinf.* **2019**, *75*, 171–181. [[CrossRef](#)]
109. Govind, N.R.; Ramesh, H. The impact of spatiotemporal patterns of land use land cover and land surface temperature on an urban cool island: A case study of Bengaluru. *Environ. Monit. Assess.* **2019**, *191*, 283. [[CrossRef](#)]
110. Nimish, G.; Bharath, H.; Lalitha, A. Exploring temperature indices by deriving relationship between land surface temperature and urban landscape. *Remote Sens. Appl. Soc. Environ.* **2020**, *18*, 100299. [[CrossRef](#)]
111. Santamouris, M. Recent progress on urban overheating and heat island research. Integrated assessment of the energy, environmental, vulnerability and health impact. Synergies with the global climate change. *Energy Build.* **2020**, *207*, 109482. [[CrossRef](#)]
112. Xue, T.; Zhu, T.; Zheng, Y.; Zhang, Q. Declines in mental health associated with air pollution and temperature variability in China. *Nat. Commun.* **2019**, *10*, 2165. [[CrossRef](#)]
113. Yu, Z.; Jing, Y.; Yang, G.; Sun, R. A New Urban Functional Zone-Based Climate Zoning System for Urban Temperature Study. *Remote Sens.* **2021**, *13*, 251. [[CrossRef](#)]
114. Gómez-Baggethun, E.; Gren, Å.; Barton, D.N.; Langemeyer, J.; McPhearson, T.; O'Farrell, P.; Andersson, E.; Hamstead, Z.; Kremer, P. Urban Ecosystem Services. In *Urbanization, Biodiversity and Ecosystem Services: Challenges and Opportunities*; Springer: Dordrecht, The Netherlands, 2013; pp. 175–251. [[CrossRef](#)]
115. Zhang, Y.; Zhao, L.; Liu, J.; Liu, Y.; Li, C. The Impact of Land Cover Change on Ecosystem Service Values in Urban Agglomerations along the Coast of the Bohai Rim, China. *Sustainability* **2015**, *7*, 10365–10387. [[CrossRef](#)]
116. Gong, J.; Li, J.; Yang, J.; Li, S.; Tang, W. Land Use and Land Cover Change in the Qinghai Lake Region of the Tibetan Plateau and Its Impact on Ecosystem Services. *Int. J. Environ. Res. Public Health* **2017**, *14*, 818. [[CrossRef](#)] [[PubMed](#)]
117. Llambí, L.D.; Becerra, M.T.; Peralvo, M.; Avella, A.; Baruffol, M.; Díaz, L.J. Monitoring Biodiversity and Ecosystem Services in Colombia's High Andean Ecosystems: Toward an Integrated Strategy. *Mt. Res. Dev.* **2019**, *39*, 81–85. [[CrossRef](#)]
118. Hein, L.; van Koppen, K.; de Groot, R.S.; van Ierland, E.C. Spatial scales, stakeholders and the valuation of ecosystem services. *Ecol. Econ.* **2006**, *57*, 209–228. [[CrossRef](#)]
119. Estoque, R.C.; Murayama, Y. Examining the potential impact of land use/cover changes on the ecosystem services of Baguio city, the Philippines: A scenario-based analysis. *Appl. Geogr.* **2012**, *35*, 316–326. [[CrossRef](#)]
120. Miles, L.; Kapos, V. Reducing Greenhouse Gas Emissions from Deforestation and Forest Degradation: Global Land-Use Implications. *Science* **2008**, *320*, 1454–1455. [[CrossRef](#)]
121. Shuaib, A.; Rana, M.P. Assessing water supply for the urban poor in Rajshahi City, Bangladesh. *Manag. Environ. Qual. Int. J.* **2020**, *31*, 75–88. [[CrossRef](#)]
122. Köppen, W. Klassifikation der Klimate nach Temperatur, Niederschlag und Jahresablauf (Classification of Climates According to Temperature, Precipitation and Seasonal Cycle). *Petermanns Geogr. Mitt.* **1918**, *64*, 193–203.
123. Rahman, M.T.U.; Habib, A.; Tasnim, R.; Khan, M.F. Impact of Climate Change in Rajshahi City Based on Marksim Weather Generator, Temperature Projections. In *Water Security in Asia*; Springer: Cham, Switzerland, 2021; pp. 339–348. [[CrossRef](#)]
124. Islam, M.; Uddin, M.N.; Rahman, M.M. A GIS-based approach to explore the factors contributing towards Urban residential land development and re-development (LDR): A case of Rajshahi City Corporation area. *Geol. Ecol. Landsc.* **2020**, *1*–12. [[CrossRef](#)]
125. He, S.; Yu, S.; Li, G.; Zhang, J. Exploring the influence of urban form on land-use efficiency from a spatiotemporal heterogeneity perspective: Evidence from 336 Chinese cities. *Land Use Policy* **2020**, *95*, 104576. [[CrossRef](#)]
126. Singh, D.; Kumar, V. Image dehazing using Moore neighborhood-based gradient profile prior. *Signal Process. Image Commun.* **2019**, *70*, 131–144. [[CrossRef](#)]
127. Avdan, U.; Jovanovska, G. Algorithm for Automated Mapping of Land Surface Temperature Using LANDSAT 8 Satellite Data. *J. Sens.* **2016**, *2016*, 1480307. [[CrossRef](#)]
128. Zhao, Z.; Sharifi, A.; Dong, X.; Shen, L.; He, B.-J. Spatial Variability and Temporal Heterogeneity of Surface Urban Heat Island Patterns and the Suitability of Local Climate Zones for Land Surface Temperature Characterization. *Remote Sens.* **2021**, *13*, 4338. [[CrossRef](#)]
129. Rahman, M.; Szabó, G. Impact of Land Use and Land Cover Changes on Urban Ecosystem Service Value in Dhaka, Bangladesh. *Land* **2021**, *10*, 793. [[CrossRef](#)]
130. Costanza, R.; d'Arge, R.; de Groot, R.; Farber, S.; Grasso, M.; Hannon, B.; Limburg, K.; Naeem, S.; O'Neill, R.V.; Paruelo, J.; et al. The value of the world's ecosystem services and natural capital. *Nature* **1997**, *387*, 253–260. [[CrossRef](#)]
131. Hu, H.; Liu, W.; Cao, M. Impact of land use and land cover changes on ecosystem services in Menglung, Xishuangbanna, Southwest China. *Environ. Monit. Assess.* **2008**, *146*, 147–156. [[CrossRef](#)]
132. US-BLS (2021) CPI Inflation Calculator. Available online: [https://www.bls.gov/data/inflation\\_calculator.htm](https://www.bls.gov/data/inflation_calculator.htm) (accessed on 30 December 2021).
133. Li, R.-Q.; Dong, M.; Cui, J.-Y.; Zhang, L.-L.; Cui, Q.-G.; He, W.-M. Quantification of the Impact of Land-Use Changes on Ecosystem Services: A Case Study in Pingbian County, China. *Environ. Monit. Assess.* **2007**, *128*, 503–510. [[CrossRef](#)]
134. Kreuter, U.P.; Harris, H.G.; Matlock, M.D.; Lacey, R. Change in ecosystem service values in the San Antonio area, Texas. *Ecol. Econ.* **2001**, *39*, 333–346. [[CrossRef](#)]

135. Vicharnakorn, P.; Shrestha, R.P.; Nagai, M.; Salam, A.P.; Kiratiprayoon, S. Carbon Stock Assessment Using Remote Sensing and Forest Inventory Data in Savannakhet, Lao PDR. *Remote Sens.* **2014**, *6*, 5452–5479. [[CrossRef](#)]
136. Chuai, X.; Huang, X.; Lai, L.; Wang, W.; Peng, J.; Zhao, R. Land use structure optimization based on carbon storage in several regional terrestrial ecosystems across China. *Environ. Sci. Policy* **2013**, *25*, 50–61. [[CrossRef](#)]
137. Iqbal, A.; Hossen, S.; Islam, M.N. Soil organic carbon dynamics for different land uses and soil management practices in Mymensingh. In Proceedings of the 5th International Conference on Environmental Aspects of Bangladesh [ICEAB 2014], Dhaka, Bangladesh, 23–24 May 2014.
138. Islam, R.; Rahman, L.; Islam, D.; Kashem, A.; Satter, A.; Bokhtiar, S.; Hossain, B.; Rahman, M. Assessment of carbon stock and nutrient contents in soils of Northern and Eastern piedmont plains of Bangladesh. *SAARC J. Agric.* **2019**, *16*, 61–72. [[CrossRef](#)]
139. Saha, P.; Rahman, M.; Khatun, M.; Hossain, A.; Saleque, M. Assessment of soil carbon stock of some selected agroecological zones of Bangladesh. *Bangladesh J. Agric. Res.* **2014**, *38*, 625–635. [[CrossRef](#)]
140. Nayak, D.R.; Saetnan, E.; Cheng, K.; Wang, W.; Koslowski, F.; Cheng, Y.-F.; Zhu, W.Y.; Wang, J.-K.; Liu, J.-X.; Moran, D.; et al. Management opportunities to mitigate greenhouse gas emissions from Chinese agriculture. *Agric. Ecosyst. Environ.* **2015**, *209*, 108–124. [[CrossRef](#)]
141. Goetz, S.J.; Baccini, A.; Laporte, N.T.; Johns, T.; Walker, W.; Kellndorfer, J.; Houghton, R.A.; Sun, M. Mapping and monitoring carbon stocks with satellite observations: A comparison of methods. *Carbon Balance Manag.* **2009**, *4*, 2. [[CrossRef](#)] [[PubMed](#)]
142. Bindu, G.; Rajan, P.; Jishnu, E.; Joseph, K.A. Carbon stock assessment of mangroves using remote sensing and geographic information system. *Egypt. J. Remote Sens. Space Sci.* **2018**, *23*, 1–9. [[CrossRef](#)]
143. Situmorang, J.P.; Sugianto, S. Estimation of Carbon Stock Stands using EVI and NDVI Vegetation Index in Production Forest of Lembah Seulawah Sub-District, Aceh Indonesia. *Aceh Int. J. Sci. Technol.* **2016**, *5*, 126–139. [[CrossRef](#)]
144. Liu, H.Q.; Huete, A. A feedback based modification of the NDVI to minimize canopy background and atmospheric noise. *IEEE Trans. Geosci. Remote Sens.* **2019**, *33*, 457–465. [[CrossRef](#)]
145. Huete, A.R.; Liu, H.Q.; Batchily, K.V.; van Leeuwen, W. A comparison of vegetation indices over a global set of TM images for EOS-MODIS. *Remote Sens. Environ.* **1997**, *59*, 440–451. [[CrossRef](#)]
146. Gemitzi, A.; Tsihrintzis, V.A.; Voudrias, E.; Petalas, C.; Stravodimos, G. Combining geographic information system, multicriteria evaluation techniques and fuzzy logic in siting MSW landfills. *Environ. Earth Sci.* **2007**, *51*, 797–811. [[CrossRef](#)]
147. Radočaj, D.; Jurišić, M.; Gašparović, M.; Plaščak, I. Optimal Soybean (*Glycine max* L.) Land Suitability Using GIS-Based Multicriteria Analysis and Sentinel-2 Multitemporal Images. *Remote Sens.* **2020**, *12*, 1463. [[CrossRef](#)]
148. Yin, S.; Li, J.; Liang, J.; Jia, K.; Yang, Z.; Wang, Y. Optimization of the Weighted Linear Combination Method for Agricultural Land Suitability Evaluation Considering Current Land Use and Regional Differences. *Sustainability* **2020**, *12*, 10134. [[CrossRef](#)]
149. Boroushaki, S.; Malczewski, J. Implementing an extension of the analytical hierarchy process using ordered weighted averaging operators with fuzzy quantifiers in ArcGIS. *Comput. Geosci.* **2008**, *34*, 399–410. [[CrossRef](#)]
150. Luan, C.; Liu, R.; Peng, S. Land-use suitability assessment for urban development using a GIS-based soft computing approach: A case study of Ili Valley, China. *Ecol. Indic.* **2021**, *123*, 107333. [[CrossRef](#)]
151. Rahman, M.; Ningsheng, C.; Islam, M.; Dewan, A.; Iqbal, J.; Washakh, R.M.A.; Shufeng, T. Flood Susceptibility Assessment in Bangladesh Using Machine Learning and Multi-criteria Decision Analysis. *Earth Syst. Environ.* **2019**, *3*, 585–601. [[CrossRef](#)]
152. Tang, Z.; Yi, S.; Wang, C.; Xiao, Y. Incorporating probabilistic approach into local multi-criteria decision analysis for flood susceptibility assessment. *Stoch. Hydrol. Hydraul.* **2018**, *32*, 701–714. [[CrossRef](#)]
153. Romano, G.; Sasso, P.D.; Liuzzi, G.T.; Gentile, F. Multi-criteria decision analysis for land suitability mapping in a rural area of Southern Italy. *Land Use Policy* **2015**, *48*, 131–143. [[CrossRef](#)]
154. Saaty, R.W. The analytic hierarchy process—What it is and how it is used. *Math. Model.* **1987**, *9*, 161–176. [[CrossRef](#)]
155. Diakoulaki, D.; Mavrotas, G.; Papayannakis, L. Determining objective weights in multiple criteria problems: The critic method. *Comput. Oper. Res.* **1995**, *22*, 763–770. [[CrossRef](#)]
156. Olsen, A.A.; Wolcott, M.D.; Haines, S.T.; Janke, K.K.; McLaughlin, J.E. How to use the Delphi method to aid in decision making and build consensus in pharmacy education. *Curr. Pharm. Teach. Learn.* **2021**, *13*, 1376–1385. [[CrossRef](#)]
157. Rahman, M.; Szabó, G. A Geospatial Approach to Measure Social Benefits in Urban Land Use Optimization Problem. *Land* **2021**, *10*, 1398. [[CrossRef](#)]
158. Saaty, T.L. How to make a decision: The analytic hierarchy process. *Eur. J. Oper. Res.* **1990**, *48*, 9–26. [[CrossRef](#)]
159. Li, X.; Ma, X. An improved simulated annealing algorithm for interactive multi-objective land resource spatial allocation. *Ecol. Complex.* **2018**, *36*, 184–195. [[CrossRef](#)]
160. Basu, A.; Das, S. Afforestation, revegetation, and regeneration: A case study on Purulia district, West Bengal (India). In *Modern Cartography Series*; Academic Press: Cambridge, MA, USA, 2021; pp. 497–524. [[CrossRef](#)]
161. Imran, H.M.; Hossain, A.; Islam, A.K.M.S.; Rahman, A.; Bhuiyan, A.E.; Paul, S.; Alam, A. Impact of Land Cover Changes on Land Surface Temperature and Human Thermal Comfort in Dhaka City of Bangladesh. *Earth Syst. Environ.* **2021**, *5*, 667–693. [[CrossRef](#)]
162. Voogt, J.A.; Oke, T.R. Thermal remote sensing of urban climates. *Remote Sens. Environ.* **2003**, *86*, 370–384. [[CrossRef](#)]
163. Palafox-Juárez, E.; López-Martínez, J.; Hernández-Stefanoni, J.; Hernández-Núñez, H. Impact of Urban Land-Cover Changes on the Spatial-Temporal Land Surface Temperature in a Tropical City of Mexico. *ISPRS Int. J. Geo Inf.* **2021**, *10*, 76. [[CrossRef](#)]

164. Mensah, C.; Atayi, J.; Kabo-Bah, A.T.; Švik, M.; Acheampong, D.; Kyere-Boateng, R.; Prempeh, N.A.; Marek, M.V. Impact of urban land cover change on the garden city status and land surface temperature of Kumasi. *Cogent Environ. Sci.* **2020**, *6*, 1787738. [[CrossRef](#)]
165. Igun, E.; Williams, M. Impact of urban land cover change on land surface temperature. *Glob. J. Environ. Sci. Manag.* **2018**, *4*, 47–58. [[CrossRef](#)]
166. Naughton, J.; McDonald, W. Evaluating the Variability of Urban Land Surface Temperatures Using Drone Observations. *Remote Sens.* **2019**, *11*, 1722. [[CrossRef](#)]
167. Yang, J.; Wong, M.S.; Menenti, M.; Nichol, J. Study of the geometry effect on land surface temperature retrieval in urban environment. *ISPRS J. Photogramm. Remote Sens.* **2015**, *109*, 77–87. [[CrossRef](#)]
168. Lukáč, J.; Mihalčová, B.; Manová, E.; Kozel, R.; Vilamova, Š.; Čulková, K. The position of the Visegrád countries by clustering methods based on indicator environmental performance index. *Ekol. Bratislava.* **2020**, *39*, 16–26. [[CrossRef](#)]
169. Široka, M.; Piličić, S.; Milošević, T.; Lacalle, I.; Traven, L. A novel approach for assessing the ports' environmental impacts in real time—The IoT based port environmental index. *Ecol. Indic.* **2021**, *120*, 106949. [[CrossRef](#)]
170. Zhou, P.; Delmas, M.; Kohli, A. Constructing meaningful environmental indices: A nonparametric frontier approach. *J. Environ. Econ. Manag.* **2017**, *85*, 21–34. [[CrossRef](#)]
171. Qin, Y.; Qi, Q.; Scott, P.J.; Jiang, X. Multiple criteria decision making based on weighted Archimedean power partitioned Bonferroni aggregation operators of generalised orthopair membership grades. *Soft Comput.* **2020**, *24*, 12329–12355. [[CrossRef](#)]
172. Liu, P.; Zhang, X. A Multicriteria Decision-Making Approach with Linguistic D Numbers Based on the Choquet Integral. *Cogn. Comput.* **2019**, *11*, 560–575. [[CrossRef](#)]